IN THE UNITED STATES PATENT AND TRADEMARK OFFICE

In re Application of:

Tabin et al.

Serial No: 08/905,572

Filed: August 1, 1997

For: Methods and Compositions for Regulating Skeletogenic Formation

Art Unit: 1646

Attorney Docket No. HMSU-P07-006

Examiner: C. Kaufman

Commissioner for Patents
Washington, DC 20231

Declaration Under 35 U.S.C. §1.132 of Lee Rubin

Sir:

I, Lee Rubin of Massachusetts, hereby declare as follows:

1. I am an employee of Curis Inc., which licenses the above-described application from Harvard Medical School, the assignee of record.

2. Experiments were performed in collaboration with me, the results of which are depicted in Exhibits A-J, which demonstrate the effects of treating adult tissues with *sonic hedgehog* or *indian hedgehog*. Exhibits A-D summarize the effects of *sonic hedgehog* or *indian hedgehog* on adult bovine cartilage explants grown in 3-dimensional culture in a bioreactor. Exhibit A shows that treatment of these cartilage explants with either *sonic hedgehog* or *indian hedgehog* increases the weight of the explants following four weeks in culture. Exhibit B shows that treatment of adult bovine cartilage explants with either *sonic hedgehog* or *indian hedgehog* increases the cell number in the explants following four weeks in culture. Exhibit C shows that treatment with either *sonic hedgehog* or *indian hedgehog* increases GAG content in explants following four weeks in culture. Exhibit D shows pictures of the cartilage explants following four weeks in culture and demonstrates that explants treated with *sonic hedgehog* resemble and are larger than control explants treated with BMP or IGF. Each of these experiments demonstrates that treatment of adult cartilage tissue with either *sonic hedgehog* or *indian hedgehog* increases the growth and proliferation of the tissue.

Exhibits E-L summarize the effects of systemic delivery of *sonic hedgehog* (either lipid modified or unmodified) to either young mice or adult mice. Exhibits E-F demonstrate that systemic delivery of *sonic hedgehog* to D11 mice induces expression of *patched-1*, as well as

EXHIBIT 5

expansion of the growth plate. Exhibit G shows the results of BrdU staining and indicates that systemic delivery of *sonic hedgehog* induces chondrocyte proliferation in the growth plate of D11 mice. Exhibits H-L show that, similarly to the results obtained upon systemic administration of *sonic hedgehog* to D11 mice, administration of *sonic hedgehog* to the knee joint of either skeletally mature or aged adult mice results in both the induction of *patched-1* expression and an increase in proliferation. Each of these experiments demonstrate the *in vivo* efficacy of *sonic hedgehog* on cartilage of both young mice and adult mice.

3. The above experiments were performed in accord with the teachings of the abovementioned patent application.

4. I hereby declare that all statements made herein of my own knowledge are true and that all statements made on information and belief are believed to be true; and further that these statements are made with knowledge that willful false statements and the like so made are punishable by fine or imprisonment, or both, under Section 1001 of Title XVIII of the United States Code and that willful false statements may jeopardize the validity of this Application for Patent or any patent issuing thereon.

Lee Rubin

Dated: _____ Signature:

Wet weight / construct (1% serum)

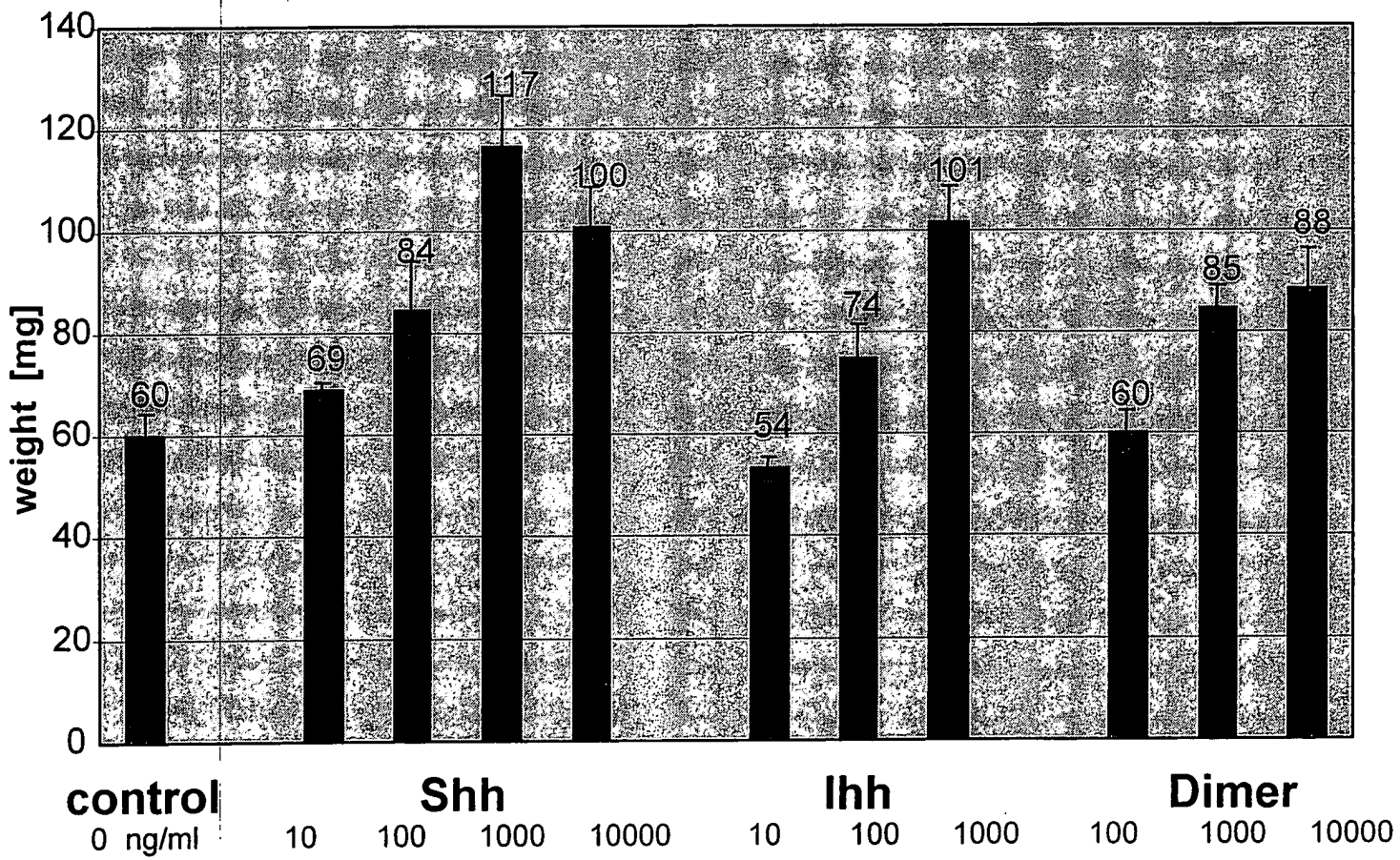

Cell number / dry weight (1% serum)

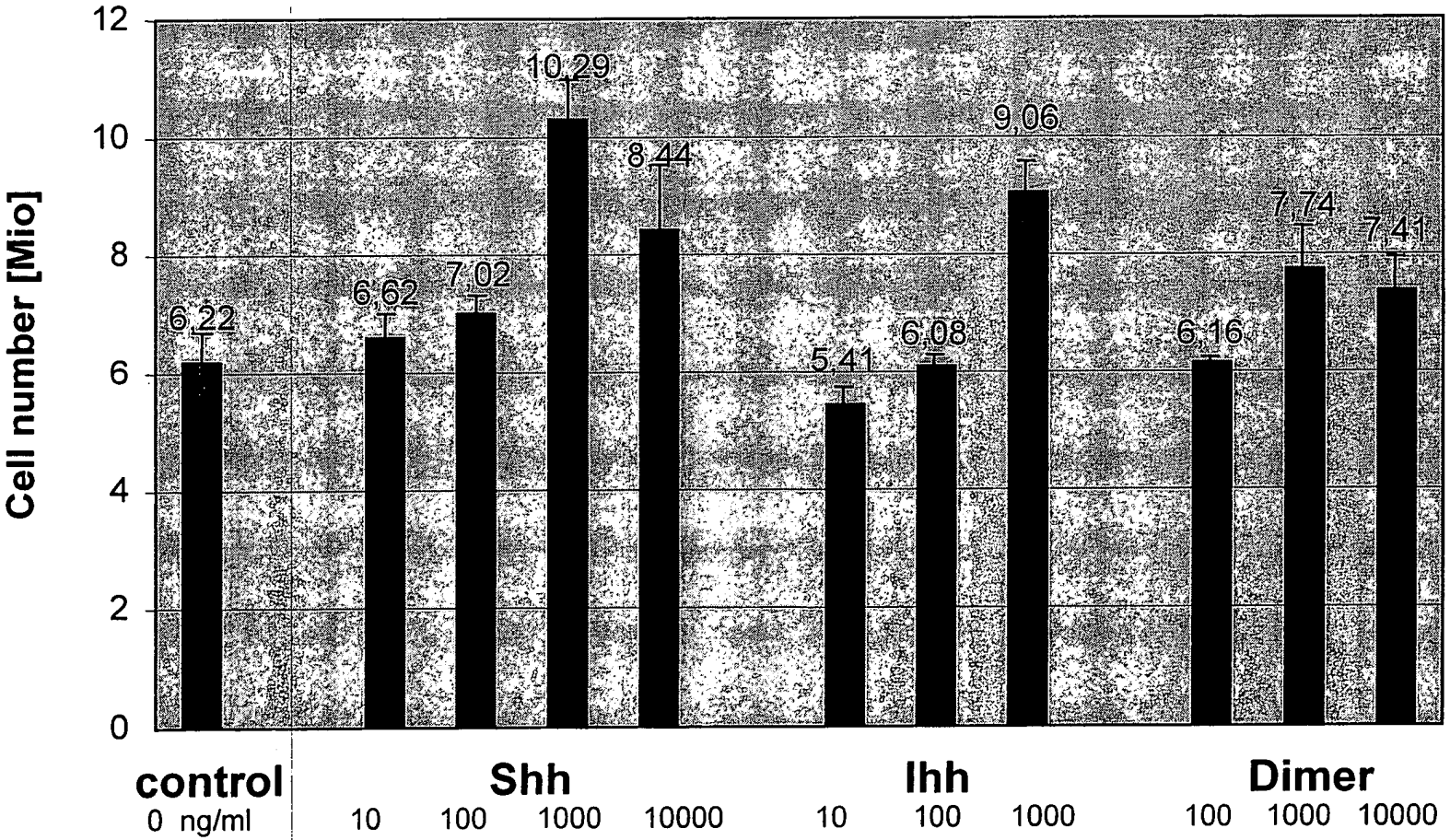

GAG / cell (1% serum)

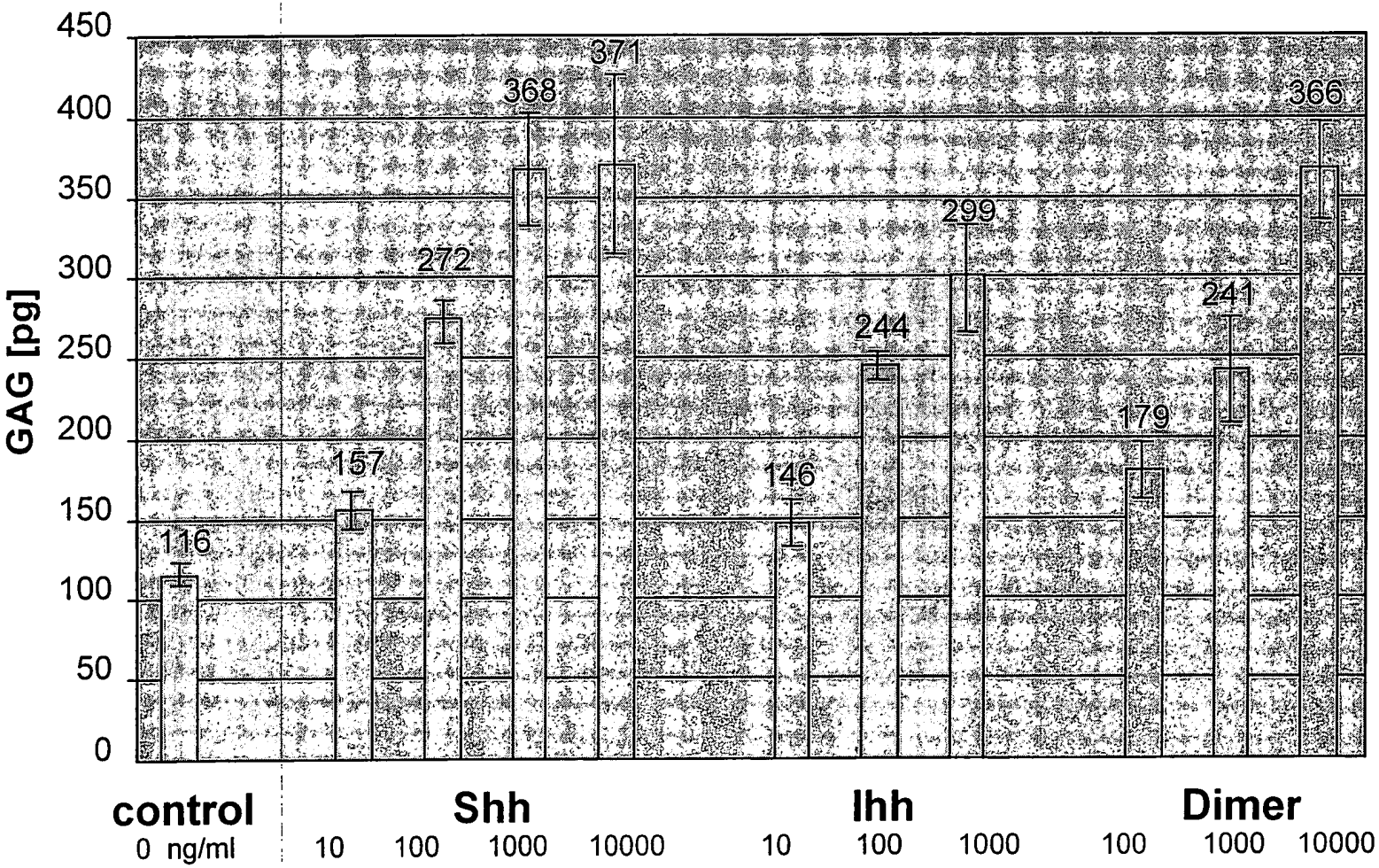

Constructs after 4 weeks of culture (in 1% serum)

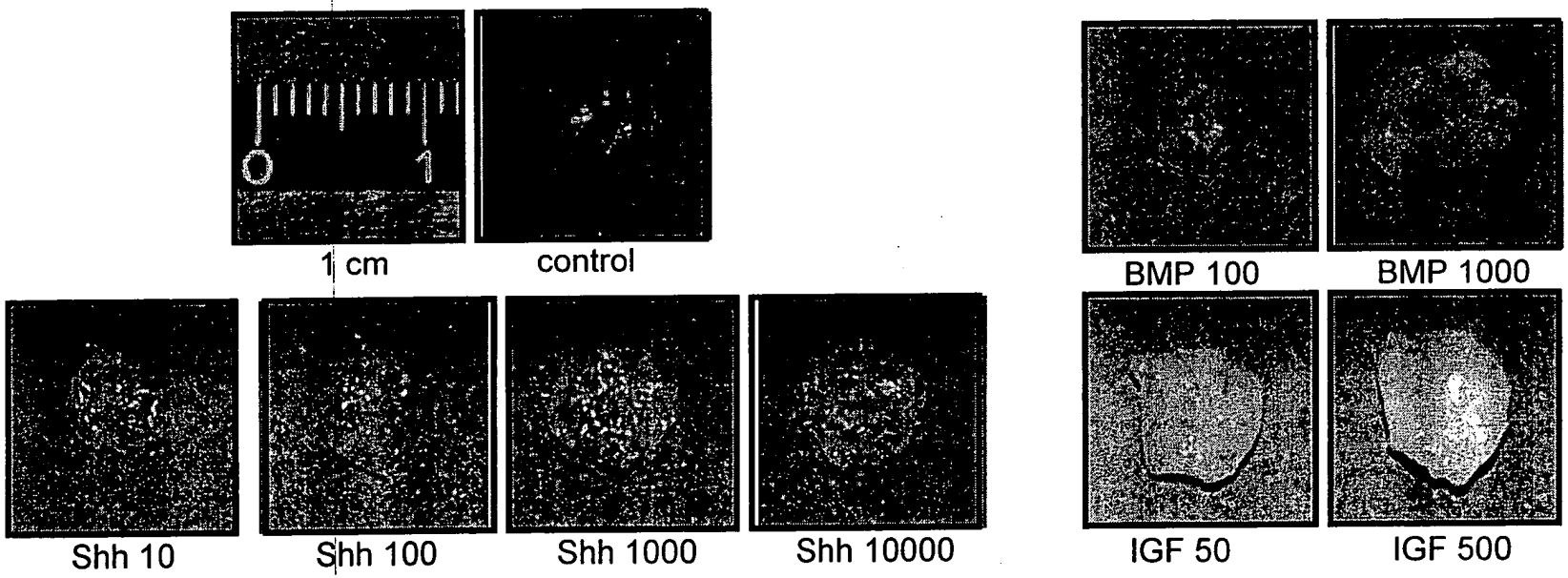

In vivo effects of Hh protein

Systemic delivery of Shh in young mice induces *Ptc-1* expression (D11 mice) and growth plate expansion

Shh or pyr-Shh 10 mg/Kg

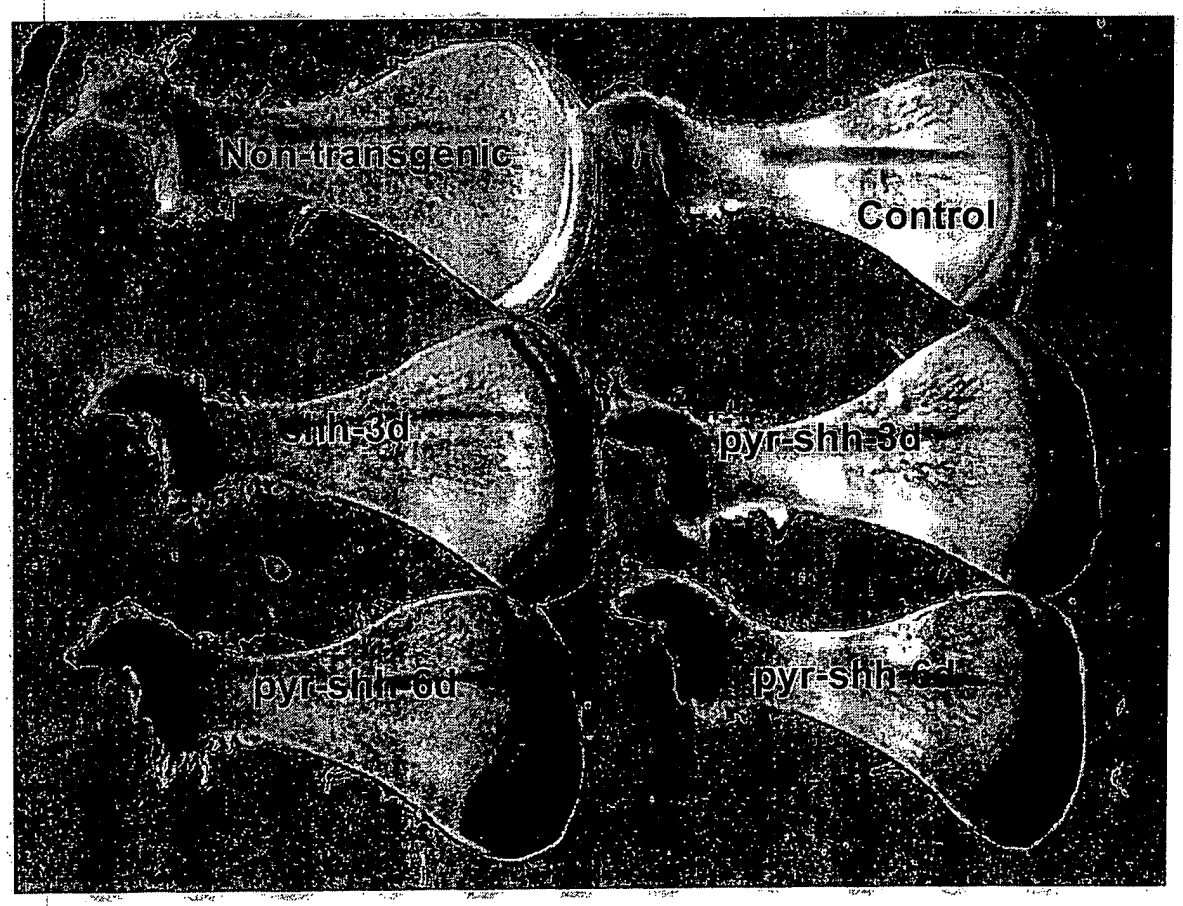

Systemic delivery of Shh in young mice induces growth plate expansion

pyr-Shh
10 mg/Kg

(Alcian blue wholemount)

Vehicle

dipal-Shh

Systemic delivery of octyl-Shh (10 mg/Kg, 2.5 days) induces chondrocyte proliferation in the growth plate growing mice

BrdU immunostain

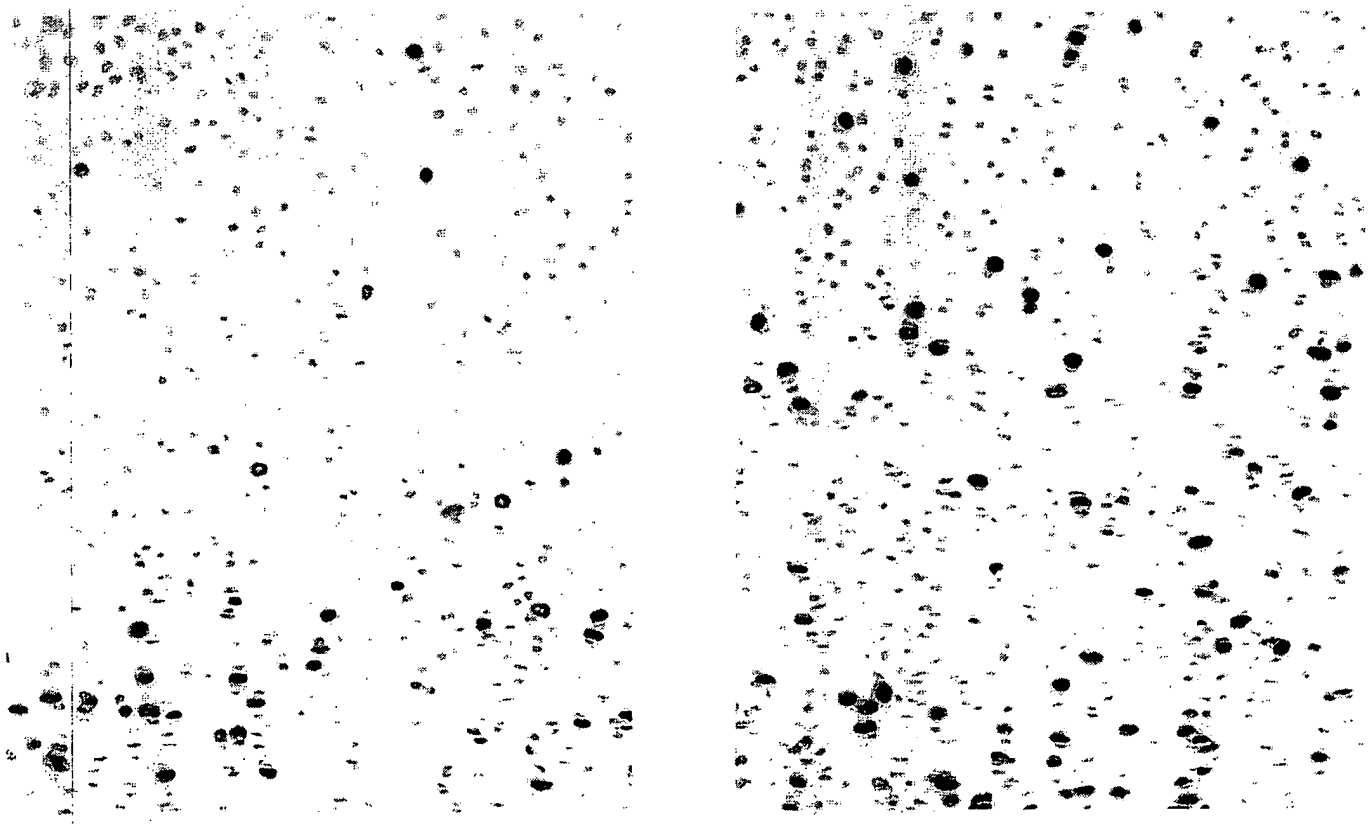

Vehicle **dipal-Shh**

In vivo effects of Shh on articular cartilage

Intra-articular injections of dipal-Shh into the mouse knee joint

- Skeletally mature young adults or aged animals (B6 or Ptc-LacZ)
- One injection per day, 10 ml (10 mg or 30 mg)
- 3-day, 6-day and 11-day treatments
- "Recovery" period of 1, 8, 16, or 30 days

Systemic delivery of Hh protein induces *Ptc-1* expression in articular chondrocytes

+ vehicle

+ dipal-Shh

H&E stain
+
X-gal stain

Adult mouse
femoral head

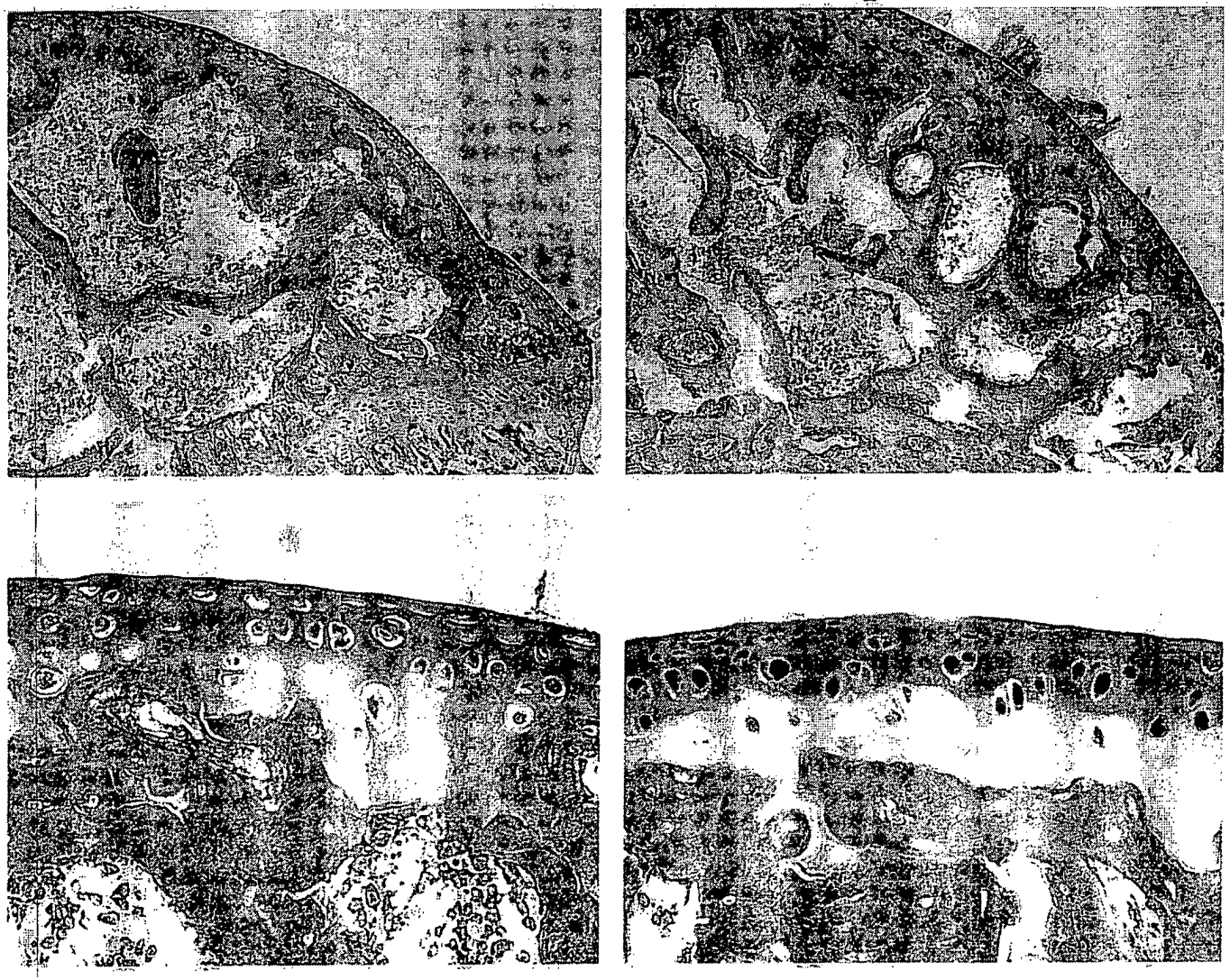

Local delivery of Hh protein induces *Ptc-1* expression in articular chondrocytes

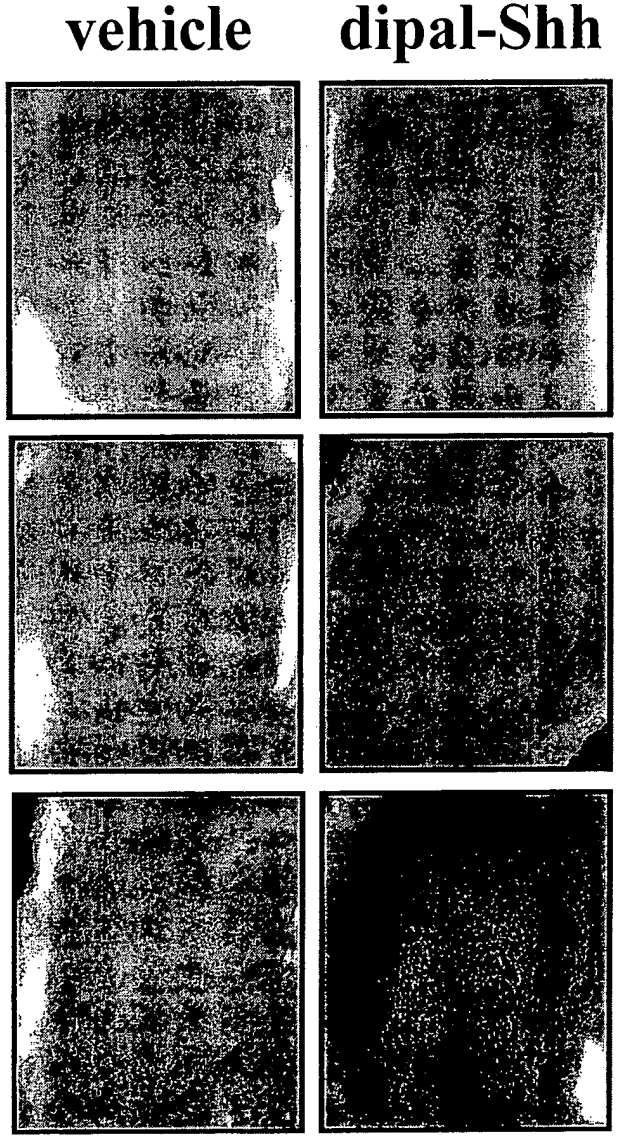

X-gal stain of patellar cartilage from adult mice

PCNA immunohistochemical assay for chondrocyte proliferation

vehicle

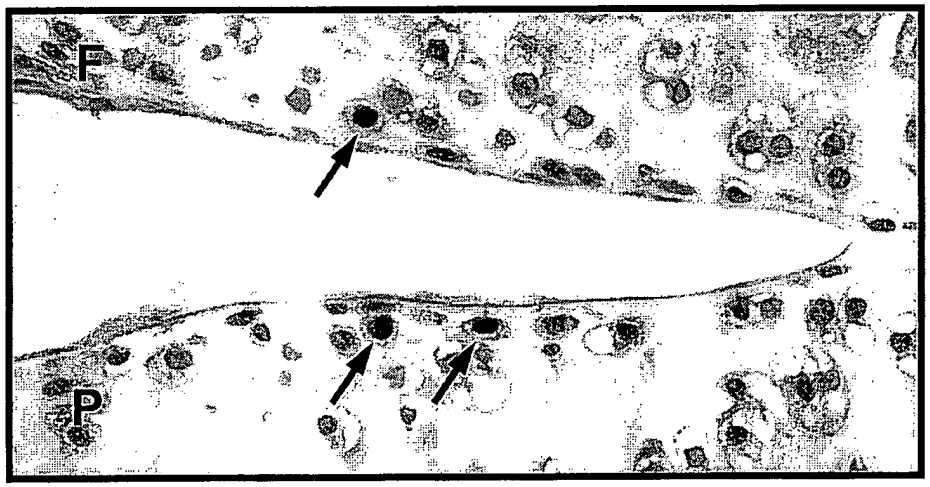

dipal-Shh
(6 inj.)

Adult
Patellofemoral
compartment
magnification
= 40X

dipal-Shh treatment induced chondrocyte proliferation in the patellar cartilage of the mouse knee joint

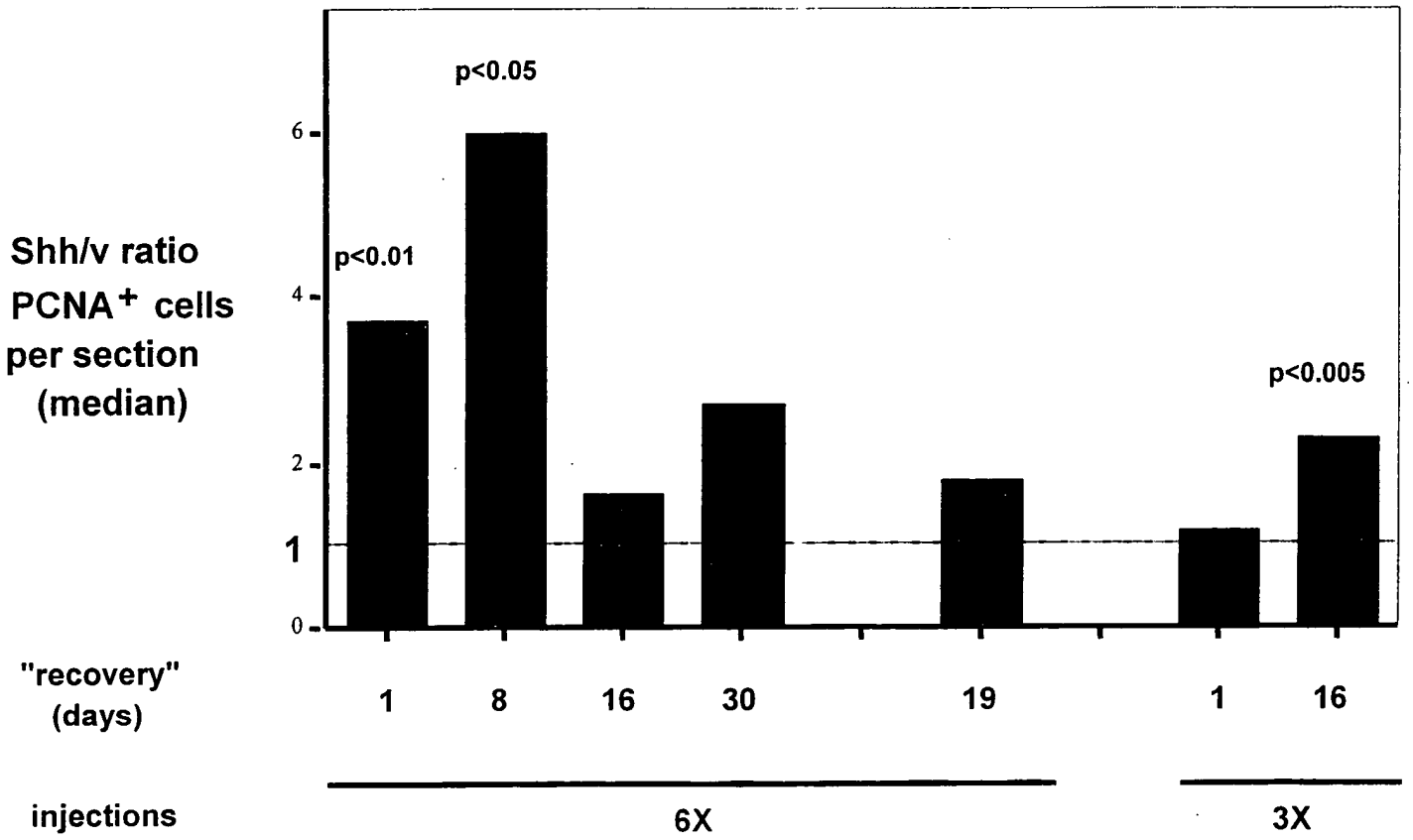

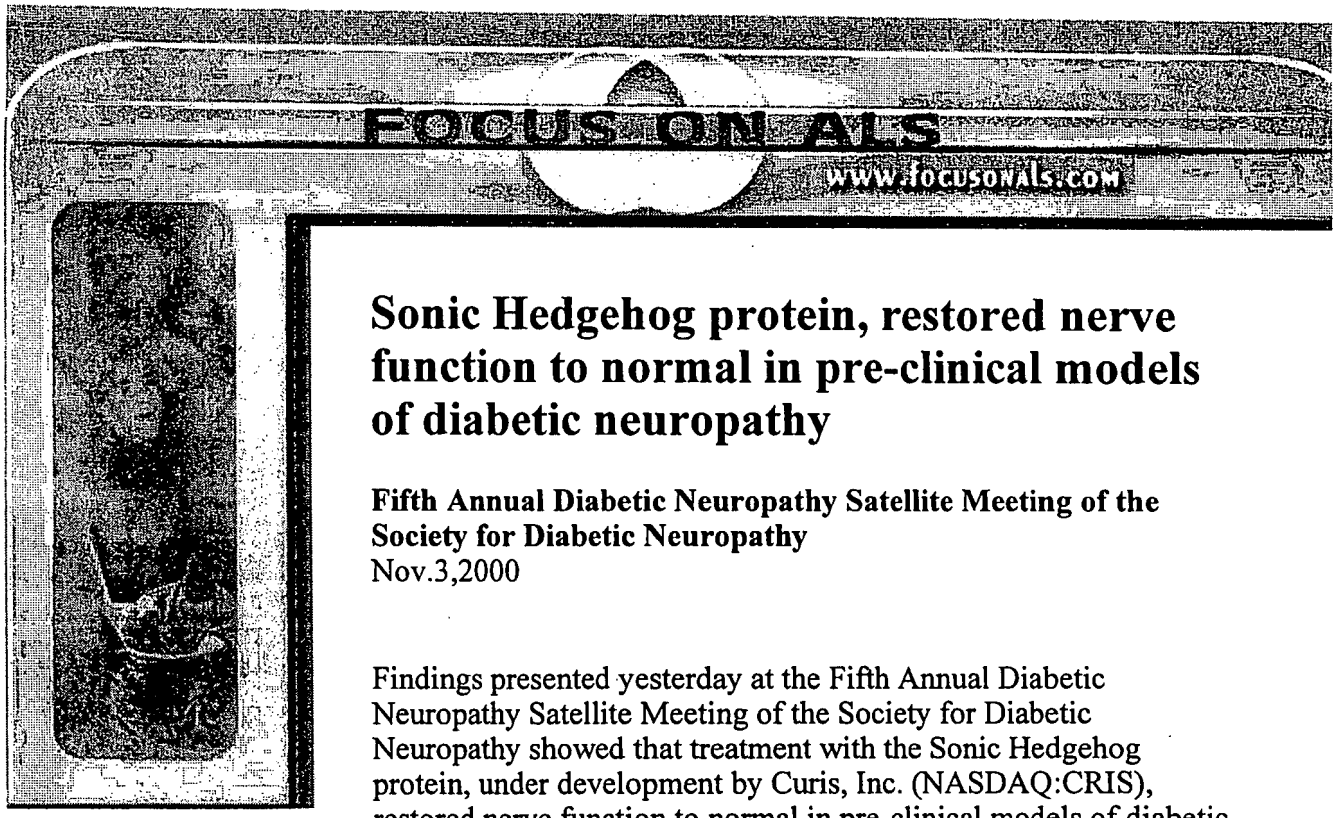

Sonic Hedgehog protein, restored nerve function to normal in pre-clinical models of diabetic neuropathy

Fifth Annual Diabetic Neuropathy Satellite Meeting of the Society for Diabetic Neuropathy
Nov.3,2000

Findings presented yesterday at the Fifth Annual Diabetic Neuropathy Satellite Meeting of the Society for Diabetic Neuropathy showed that treatment with the Sonic Hedgehog protein, under development by Curis, Inc. (NASDAQ:CRIS), restored nerve function to normal in pre-clinical models of diabetic neuropathy.

Data from a study conducted by Dr. David Tomlinson of the University of Manchester showed complete restoration of both sensory and motor nerve function in pre-clinical models after that function was impaired. Five weeks after treatment on these models was begun, nerve conduction velocity measurements showed that sensory and motor function returned to pre-diabetic levels.

"These findings are an important part of the pre-IND program for a Hedgehog-based treatment for diabetic neuropathy at Curis," said Doros Platika, M.D., president and chief executive officer of Curis. "The repair and restoration of normal function in nerves that have been compromised by diabetes, as shown in this study, represents a key objective of the company's efforts in developmental biology, and we are moving forward aggressively to move such a therapy into human clinical testing.

"Of the estimated 15 million people with diabetes in the U.S., approximately six million patients have diabetic neuropathy. The market for treatments of this condition is estimated to be $1.5 billion. Additional neurological diseases that may benefit from a Hedgehog-based therapy include multiple sclerosis, chemotherapy-induced neuropathy, Alzheimer's disease, and amyotrophic lateral sclerosis.
The family of Hedgehog proteins and their role in the development of neuronal cells and tissues are a key focus of ongoing research

Home
What Is ALS?
ALS Terms
FAQ's
ALS Facts
Symptoms
Diagnosis
Treatments
BiPAP/ CPAP
Respiratory
ALS Tips
Research
Resources
Coping
Caregiver
Communication
Nutrition
Advocacy
Links
Inspiration
Quotes
More Inspiration
PALS pal
Hospice
Hope 4 Cure
Memorial
Morrie Schwartz
My Story
Lou Gehrig
News
Top Stories
Stem Cell News

E-Cards
Profiles
E-mail
Thank you
Disclaimer

E-mail
Your comments and suggestions are welcomed and appreciated.

Guestbook FROM MediGEAR
Sign My Guestbook
View My Guestbook


"Rooster Romp"


I am a member of the HTML WRITERS GUILD

and development at Curis.

The development of innovative therapies by Curis to treat a variety of disorders, including diabetes, is focused upon recreating the conditions and redirecting key inducing molecules such as those involved in the Hedgehog pathway that control the normal growth and restore the function of tissues. Curis, Inc. is developing products based on technologies in the emerging field of regenerative medicine.

The Company is combining insights gained through the study of developmental biology with high-throughput screening capabilities, proteins, cells and biocompatible materials to facilitate the development of new regenerative medicine therapies. For more information, please visit the Curis web site.

- Air Force Base Eyed in ALS Cases
- Team finds "switch" to restore muscle
- Defective Gene Found For Amyotrophic Lateral Sclerosis With Dementia
- NIH Guidelines for research

Back to Focus On ALS Home Page
Back to Focus On ALS News Index

Back

Experimental Neurology 173, 95–104 (2002)
doi:10.1006/exnr.2001.7825, available online at http://www.idealibrary.com on IDEAL®

Intrastriatal Injection of Sonic Hedgehog Reduces Behavioral Impairment in a Rat Model of Parkinson's Disease

Kyoko Tsuboi and Clifford W. Shults

Department of Neurosciences, University of California, San Diego, La Jolla, California 92093; and Veterans Affairs Medical Center (127), 3350 La Jolla Village Drive, San Diego, California 92161

Received December 1, 2000; accepted September 14, 2001

Sonic hedgehog (Shh), a member of hedgehog (hh) family of signaling molecules, is necessary for normal axial patterning and cellular differentiation in the developing central nervous system. Shh also promotes the survival of fetal dopaminergic neurons and protects cultures of fetal midbrain dopaminergic neurons from the toxic effects of *N*-methyl-4-phenylpyridinium (MPP^+), a neurotoxin that selectively injures nigral dopaminergic neurons. The mRNA expression of Shh and its putative receptor in the adult brain indicates an important role of Shh in the mature nervous system in addition to its roles during embryogenesis. In this study we examined the behavioral and anatomical effects of intrastriatal injection of singly myristoylated wild-type human Sonic hedgehog N-terminal fragment (Shh-M) in a rat model of Parkinson's disease (PD). Five groups of rats received a series of four intrastriatal injections of Shh-M (180 ng, 540 ng, or 4.275 μg per injection), glial cell line-derived neurotrophic factor (GDNF) (1 μg/injection), or vehicle on days 1, 3, 5, and 8. On day 4, the animals received an intrastriatal injection of 15 μg 6-hydroxydopamine (6-OHDA) free base. Intrastriatal administration of Shh (180 ng/injection) twice before and after a single intrastriatal injection of 6-OHDA reduced apomorphine- and amphetamine-induced rotation and forelimb akinesia and partially preserved dopaminergic axons in the striatum. This is the first demonstration *in vivo* that Shh reduces behavioral deficits induced by intrastriatal 6-OHDA lesion and suggests that Shh may be useful in the treatment of disorders that affect the nigrostriatal system, such as PD.

Key Words: **Sonic hedgehog; Parkinson's disease; 6-hydroxydopamine; striatum; substantia nigra; tyrosine hydroxylase.**

INTRODUCTION

Parkinson's disease (PD) is a progressive neurological disorder in which the cardinal pathological feature is the loss of dopaminergic neurons in the substantia nigra pars compacta (SNpc) and their axons, which project to the striatum (16). A number of novel strategies are being explored as new therapies for PD. These include a variety of neurotrophic factors and antiapoptotic factors (40, 41), antioxidants, fetal dopaminergic cell transplantation (38), mesencephalic precursor transplantation (46), and gene therapies using adenovirus or adeno-associated virus (4, 10, 26). Glial cell line-derived neurotrophic factor (GDNF) has attracted substantial interest because of its ability to halt ongoing degeneration of dopaminergic neurons in the SNpc and to induce regeneration of dopaminergic neurons and their axons (5, 15).

Sonic hedgehog (Shh), a member of hedgehog family of signaling molecules (14, 18), is a protein with ventralizing activity that originates from the notochord and floor plate (36, 44). Shh protein is synthesized as a 45-kDa precursor protein, which is autocatalytically cleaved to yield an amino-terminal fragment of a 19-kDa peptide (N-Shh) (7). This peptide is involved in axial patterning and consequently regulates the phenotypic specification of precursor cells into functional differentiated cells (29). Using naive neural plate explants or neural tube explants derived from the appropriate levels of the rostocaudal axis, it has been shown that exposure to Shh is necessary for the induction of spinal motor neurons (29, 37, 47), midbrain dopaminergic neurons (20, 50), and basal forebrain cholinergic neurons (13). The important role of Shh during development has received increased attention since the discovery that mouse embryos lacking Shh gene function developed abnormal axial patterning in the central nervous system as well as gross atrophy of the entire cranium (9) and the recent demonstration that inhibition of Shh signaling resulted in developmental abnormalities in the cranial neural tube and branchial arches, which led to an overall reduction in head size (2). Recent studies showed that Shh acts as a gradient morphogen to control the formation of arcuate territories in the embyonic midbrain (1).

A role for Shh in processes other than development has also started to be explored. Miao *et al.* (31) showed that Shh promotes the survival of fetal dopaminergic

0014-4886/02 $35.00

EXHIBIT 7

neurons and protects cultures of fetal midbrain dopaminergic neurons from the toxic effects of *N*-methyl-4-phenylpyridinium (MPP^+), a neurotoxin that specifically injures nigral dopaminergic neurons.

The present study was designed to examine whether Shh, a multifaceted protein, prevents behavioral impairments in a rat model of PD. We examined the behavioral and anatomical effects of intrastriatal injection of singly myristoylated wild-type human Sonic hedgehog N-terminal fragment (Shh-M) on the behavioral deficits and injury to the nigrostriatal dopaminergic system caused by intrastriatal injection of 6-hydroxydopamine (6-OHDA), a neurotoxin specific for catecholaminergic neurons.

MATERIALS AND METHODS

Singly Myristoylated Wild-type Human Sonic Hedgehog N-Terminal Fragment

Wild-type human Sonic hedgehog N-terminal domain protein from Cys 24 to Gly 197 was expressed in *Escherichia coli* as a histidine-tagged fusion protein with an enterokinase cleavage site engineered into the construct immediately adjacent to Cys 24 of the mature Shh sequence. The construct sequence was confirmed by DNA sequencing. The fidelity of the final product after removal of the his tag with enterokinase and purification was confirmed by N-terminal sequencing and electrospray ionization–mass spectrometry (51). The protein was chemically myristoylated on the α-amino group on Cys 24 and repurified (48). The fidelity of the myristolyated product was verified by high-performance liquid chromatography–mass spectrometry and postsource decay measurement as previously described (35).

Intrastriatal Injections

Female Sprague–Dawley rats weighing 200–225 g were housed under a 12-h light/dark cycle with free access to food and water and cared for according to NIH guidelines. We chose to use female rather than male rats because our previous work had indicated that female rats adapted better to the harness of the rotometer and exhibited more consistent behavior when tested in the rotometers for amphetamine- and apomorphine-induced rotation.

Prior to surgical procedures, the animals were anesthetized with a mixture of ketamine, xylazine, and acepromazine. In 50 animals, cannulae (Plastic One, Roanoke, VA) were implanted in the right forebrain anterior 0.2 mm and lateral 2.5 mm from bregma (34). The cannulae, which were 22 gauge and 2.5 mm in length, terminated slightly dorsal to the corpus callosum. The animals received a series of four injections of vehicle (150 mM NaCl, 0.5 mM dithiothreitol, $n = 11$) or Shh-M at doses of 180 ng ($n = 10$), 540 ng ($n = 10$), or 4.275 μg ($n = 10$). These three doses were chosen based on the previous malonate striatal lesion model (Engber *et al.* personal communication). In the studies of Engber *et al.*, 150 and 500 ng Shh-M were both neuroprotective and 150 ng was the minimum effective dose. The highest dose that we used, 4.275 μg, was the maximum concentration possible based on the solubility of Shh-M. Shh-M and vehicle were supplied in coded vials by Biogen (Cambridge, MA), and the content of each vial was revealed at the completion of the study. Recombinant human GDNF was purchased from Peprotech (Rocky Hill, NJ) and used at a dose of 1 μg (in 150 mM NaCl, 10 mM sodium citrate, $n = 9$) per injection. The volume of injection was 1.5 μl. Using the cannula as a guide, Shh-M, GDNF, or vehicle was injected via a 10-μl Hamilton syringe with a 31-gauge needle. The injections were carried out over 5 min, and the needle was left for an additional 5 min. The animals received the injections at the following depths on the following days: day 1, 7.7 mm (ventral to skull); day 3, 7.0 mm; day 5, 7.5 mm; and day 8, 6.5 mm.

On day 4, the animals received a single intrastriatal injection of 6-OHDA at a depth of 7.0 mm ventral to skull. The 6-OHDA (22.4 μg) (RBI–Sigma, St. Louis, MO) was dissolved in 1.5 μl of 150 mM NaCl with 0.2% ascorbic acid and injected by the same procedure used for injection of Shh-M, GDNF, or vehicle.

Behavioral Evaluation

The animals were tested for apomorphine (Sigma, St. Louis, MO)- and D-amphetamine sulfate (Sigma) -induced rotational behavior weekly during weeks 2, 3, 4, and 5 following the last injection, using an automated rotometer system (San Diego Instruments, San Diego, CA). For apomorphine-induced rotation, the animals were injected subcutaneously with 0.1 mg/kg apomorphine and rotation was measured for 30 min. For D-amphetamine-induced rotation, the animals were injected subcutaneously with 1.3 mg/kg D-amphetamine and the rotation was measured for 1 h. Amphetamine-induced rotations in the last 40 min were used for further analysis, since during this time period the rotation was most consistent (data not shown). Net rotational asymmetry score was expressed as full body turns per minute and used for analysis.

Forelimb akinesia was evaluated during weeks 1 and 6 following the last injection, as described by Olsson *et al.* (33) and Kirik *et al.* (22) with some modifications. Briefly, the rat was held by the experimenter fixing its hindlimbs with one hand and the forelimb not to be monitored with the other, while the unrestrained forepaw was touching the table. The number of adjusting steps was counted while the rat was moved sideways along the table surface (90 cm in 9 s), in the forehand direction, for both forelimbs. On the 2 days preceding

the actual testing, the animals were handled in order to become familiar with the test procedure. The stepping test consisted of five trials for each forepaw, alternating between forepaws. The average of the five trials for each forepaw was calculated. The results are shown as the percentage of adjusting steps of impaired (left) forepaw to those of the normal (right) forepaw.

During week 6 following the last injection, the animals were also evaluated for open-field activity using Activity Monitor (MED Associates, Georgia, VT). The animal was put in a 42.5 cm × 42.5 cm × 30 cm Plexiglas arena in a dark room for 20 min. The distance the animal traveled, time of ambulation, time of resting, and time of stereotypy in last 15 min were used for further analyses.

Tyrosine Hydroxylase Immunohistochemistry

After all behavioral evaluations, the animals were deeply anesthetized with a mixture of ketamine, xylazine, and acepromazine and perfused with 0.9% saline, followed by ice-cold 4% paraformaldehyde in 0.1 M phosphate buffer (PB), pH 7.4. Brains were removed, postfixed overnight in 4% paraformaldehyde, and dehydrated in 18% sucrose/0.1 M PB. Coronal sections were cut at 25-μm thickness on a freezing microtome. Every eighth section was processed for free-floating tyrosine hydroxylase (TH) immunohistochemistry and adjacent sections were stained for Nissl substances.

The sections were rinsed three times in phosphate-buffered saline (PBS), quenched in 0.9% H_2O_2/1% NaOH/PBS for 20 min, and rinsed five times in PBS. After a 1-h incubation in 20% normal horse serum/0.25% Triton X-100/PBS, sections were incubated in a 1:5000 dilution of mouse anti-TH monoclonal antibody (Chemicon, Temecula, CA) for 2 nights at 4°C. After three rinses in Triton X-100/PBS, sections were incubated in a biotinylated anti-mouse IgG (Vector, Burlingame, CA) for 1 h, followed by three rinses in PBS. Finally, the sections were incubated in the avidin–biotin complex (ABC Elite) substrate (Vector) and developed with a nickel ammonium-intensified DAB reaction. After five rinses in PBS, sections were mounted on gelatin-coated slides, air-dried, dehydrated, and coverslipped with DPX mounting medium. Control experiments were carried out by omitting the primary antibodies and resulted in no tissue staining, as expected.

Histological Assessment

Quantitative histological analysis was performed using NIH 1.47 Image on a Macintosh Quadra 700 20/240 computer connected to a CCD video camera. Beginning with the section in which the corpus callosum first spanned the midline (1.6 mm anterior from bregma) in each section (200-μm intervals), the area of relatively dense tyrosine hydroxylase-immunoreactive (TH-IR) axons around the injection site (TH-IR halo) was measured. The total area of the halo of TH-IR axons of each brain was summed. The volume of the halo of TH-IR axons was estimated using the distance (200 μm) between sections. TH-IR fiber density adjacent to the injection site was evaluated on the TH-immunostained section in which the injection track appeared to be centered. The optical density of TH-IR material in 100-μm-diameter circles was taken from 12 sites adjacent to the injection track (6 sites medial to the injection track and 6-sites lateral to the injection track), using the 10X objective under the same illumination intensity. The optical density of TH-IR fibers adjacent to the injection track was expressed as a percentage of the optical density of the TH-IR fibers of the corresponding region on the intact side.

TH-IR neurons were counted in the SNpc including the substantia nigra pars lateralis (SNpl) ipsilateral and contralateral to the injection site at five levels of the mesencephalon (posterior 4.8, 5.1, 5.4, 5.7, and 6.0 mm from bregma) as previously reported (8). Since our focus was the preservation of TH-IR neurons in the injured SNpc relative to the intact side rather than the absolute number of TH-IR neurons in the SNpc, stereological counting methods were not used. We evaluated the effect of Shh-M on TH-IR neurons in the SNpc, comparing the total number of TH-IR neurons at the five levels of the SNpc on the lesioned side with that on the contralateral (unlesioned) side. Comparison of the lesioned side to the intact side of the SNpc is considered representative of the entire SNpc and has been used in a number of studies of trophic factors (40, 43, 52). The number of TH-IR neurons in the SNpc ipsilateral to the injection site was expressed as a percentage of the number in the SNpc contralateral to the injection site (42, 43). The survival analysis of treatment-dependent remaining TH-IR neurons was defined as [(remaining TH-IR neurons on the lesioned side as a percentage of the intact side in each animal in treatment group − average remaining TH-IR neurons on the lesioned side as a percentage of the intact side in the vehicle-treated group)/average loss of TH-IR neurons on the lesioned side as a percentage of the intact side in the vehicle-treated group] × 100. For example, when the average percentage of remaining TH-IR neurons in the vehicle-treated group is 61.6% and the animals in the treatment group have 75% remaining TH neurons on the lesioned side, [(75% − 61.6%)/38.4%] × 100. All anatomical studies were performed by an evaluator unaware of the assignment of the treatment group.

Statistical Analysis

All values are expressed as means ± SEM. Differences among means were analyzed by application of one-factor analysis of variance (ANOVA) for anatomical studies or two-factor repeated-measures ANOVA

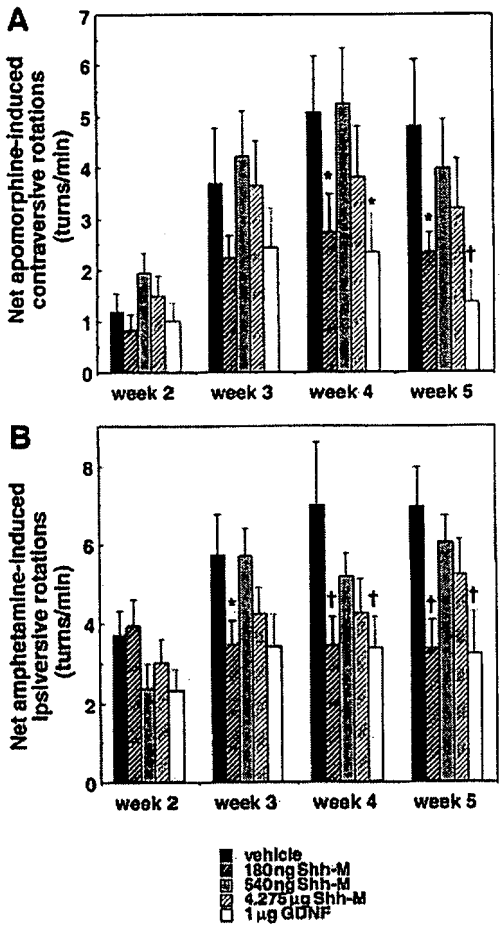

FIG. 1. Drug-induced rotations with apomorphine (0.1 mg/kg) (A) and D-amphetamine (1.3 mg/kg) (B). Values are means ± SEM (n = 10 in the three groups treated with Shh-M, n = 11 in the vehicle-treated group, n = 9 in the GDNF-treated group). Two-factor repeated-measures ANOVA (treatment × time) was used for statistical analysis. *$P < 0.05$ and †$P < 0.01$ versus the vehicle-treated group.

for behavioral studies, unless otherwise indicated. Because the study was designed to compare the effects of three doses of Shh to both a negative control (vehicle) and a positive control (GDNF), all five treatment groups were included in the ANOVA. When ANOVA showed significant differences, a pairwise comparison between means was tested by Fisher's LSD test.

RESULTS

Shh-M Attenuated Behavioral Deficits

Comparison of apomorphine-induced rotation among the five treatment groups over the four testing sessions revealed a significant treatment effect ($F_{(4, 219)} = 5.93$, $P < 0.001$, Fig. 1A). At weeks 4 and 5, apomorphine-induced rotation was significantly lower in the groups treated with GDNF and the lowest dose of Shh-M than in the vehicle-treated group. The rotation in the group treated with lowest dose of Shh-M was not significantly different from that in the GDNF-treated group at weeks 4 and 5. Comparison of amphetamine-induced rotation among the five treatment groups over the four testing sessions also revealed a significant treatment effect ($F_{(4, 219)} = 7.68$, $P < 0.001$, Fig. 1B). Amphetamine-induced behavior was significantly lower in the group treated with lowest dose of Shh-M at weeks 3, 4, and 5 and in the GDNF-treated group at weeks 4 and 5 when compared with the vehicle-treated group. There was no significant difference in amphetamine-induced rotation at weeks 4 and 5 between the groups treated with the lowest dose of Shh and the GDNF-treated group.

Comparison of forelimb akinesia among the five treatment groups over the two testing sessions also revealed a significant treatment effect ($F_{(4, 109)} = 4.33$, $P < 0.01$, Fig. 2). Similar to apomorphine- and amphetamine-induced rotation, forelimb akinesia was less severe in the GDNF-treated group and the group treated with the lowest dose of Shh-M than in the vehicle-treated group at weeks 1 and 6. The group treated with the highest dose of Shh-M also had less severe forelimb akinesia than the vehicle-treated group at week 6.

In open-field activity tests, the distance traveled by the three groups treated with Shh-M was not significantly different from that traveled by the vehicle-treated group. The GDNF-treated group traveled significantly farther than the vehicle-treated group ($F_{(4, 49)} = 4.91$, $P < 0.01$, Fig. 3A). There was no difference among the Shh-M-treated groups and the vehicle-treated group in the time of ambulation and the time of resting (Figs. 3B and 3C), whereas the GDNF-treated group was significantly different than the vehicle-treated group (time of ambulation, $F_{(4, 49)} =$

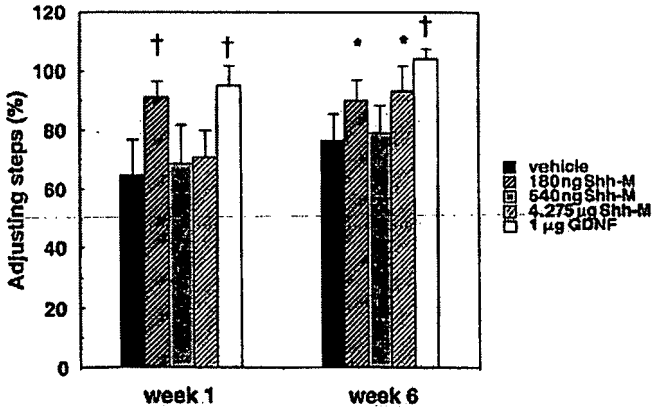

FIG. 2. Forelimb akinesia was assessed at weeks 1 and 6 after completion of a series of injections. The results are shown as the percentage of adjusting steps of impaired (left) forepaw to those of the normal (right) forepaw. Two-factor repeated-measures ANOVA (treatment × time) was used for statistical analysis. *$P < 0.05$ and †$P < 0.01$ versus the vehicle-treated group.

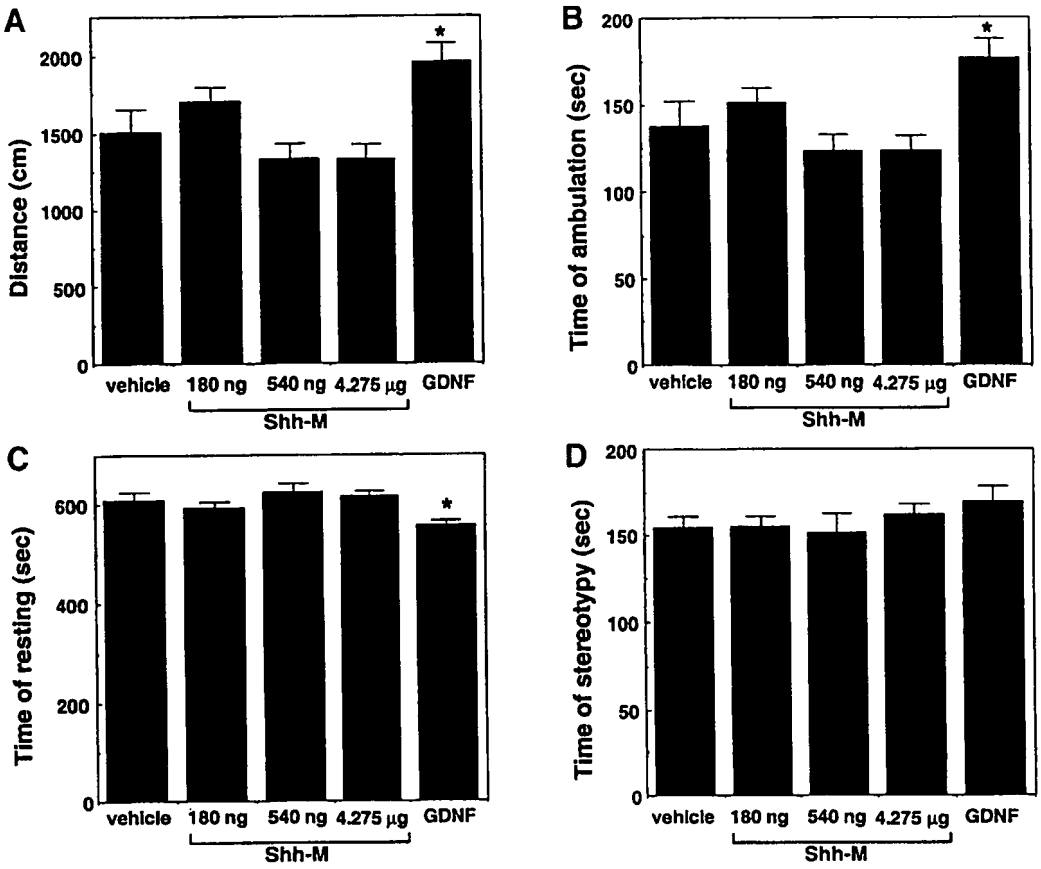

FIG. 3. Open-field activity, measured by four parameters: (A) the distance the animal traveled, (B) time of resting, (C) time of stereotypy, and (D) time of ambulation. Values are means ± SEM (n was described in the legend to Fig. 1). *$P < 0.05$ versus the vehicle-treated group.

3.79, $P < 0.01$, Fig. 3B; time of resting, $F_{(4, 49)} = 3.35$, $P < 0.05$, Fig. 3C). There was no difference in the time of stereotypy among all five groups ($F_{(4, 49)} = 0.71$, $P = 0.59$, Fig. 3D).

Comparison of body weight revealed no difference among the five groups throughout the experiment (days 1, 3, 4, 5, and 8, weeks 2 to 5; data not shown).

Shh-M Partially Spared TH-IR Fibers Adjacent to Injection Site

Spared TH-IR fibers adjacent to the needle track were observed within the area that was affected by 6-OHDA (Fig. 4). Comparison of the total area of the TH-IR halo among the five groups revealed significant differences ($F_{(4, 49)} = 27.2$, $P < 0.001$, Fig. 5A). The total area of TH-IR halo was significantly larger in both the group treated with the lowest dose of Shh-M and the GDNF-treated group than in the vehicle-treated group. The total area of TH-IR halo in the GDNF-treated group was significantly different from that in the groups treated with vehicle or Shh-M. The estimated volume of TH-IR halo was significantly greater in the GDNF-treated group (0.43 ± 0.05 mm^3) and the group treated with the lowest dose of Shh-M (0.14 ± 0.03 mm^3) than in the vehicle-treated group (0.06 ± 0.02 mm^3) ($F_{(4, 49)} = 29.0$, $P < 0.001$).

The density of TH-IR fibers along the needle track differed significantly among the groups ($F_{(4, 49)} = 17.4$, $P < 0.001$, Fig. 5B). The density of TH-IR fibers along the needle track in the GDNF-treated group was significantly higher than in the vehicle-treated group. In contrast, the density in the group treated with the lowest dose of Shh was greater than that in the vehicle-treated group but the difference did not reach statistical significance.

Shh-M Did Not Attenuate the Loss of TH-IR Neurons in SNpc

Comparison of the number of TH-IR neurons in the SNpc ipsilateral to the injection as a percentage of the number on the intact side revealed that the group treated with the lowest dose of Shh had a modest preservation of TH-IR neurons. Only the group treated with GDNF had substantial preservation (Fig. 6A); this difference reached only borderline significance ($F_{(4, 49)} = 2.45$, $P = 0.06$) because of moderately large variance in the groups. However, the survival analysis on treatment-dependent remaining TH-IR neurons

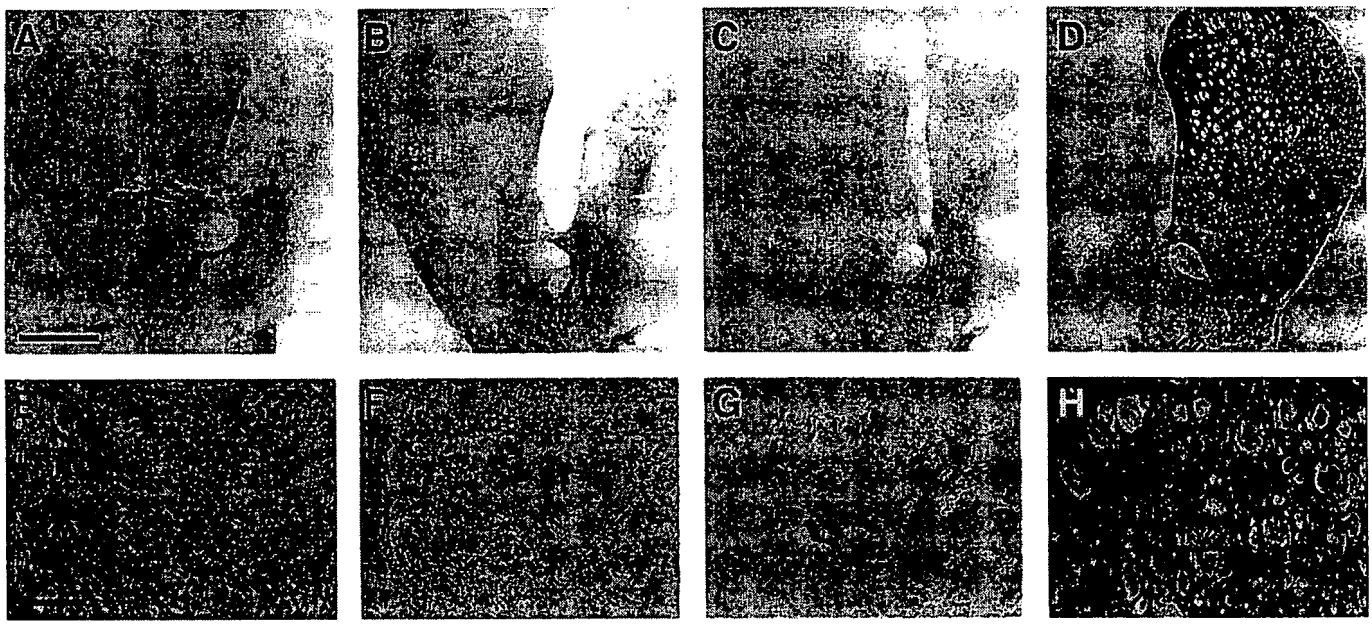

FIG. 4. Representative halo of denser TH-IR fibers around the injection site in the lesioned striatum from an animal that received GDNF at 1 μg/injection (A), Shh-M at 180 ng/injection (B), or vehicle (C). Representative unlesioned striatum (D) is the contralateral side from the vehicle-injected animal (C). Scale bar in A represents 1 mm; it applies to B–D. A significantly larger halo was observed in the GDNF-treated group and the group treated with Shh-M at 180 ng/injection than in the vehicle-treated group. High magnification of TH-IR fibers around the injection site (medial to injection site). E corresponds to A, F to B, G to C, and H to D. Scale bar in E represents 100 μm; it applies to F–H.

showed that only the GDNF-treated group was statistically different from the control (t test, $P < 0.001$, Fig. 6B).

DISCUSSION

We have demonstrated that intrastriatal injections of Shh-M at a dose of 180 ng/injection reduced behavioral impairment in three independent behavior tests: apomorphine-induced rotation, amphetamine-induced rotation, and the stepping test. We have also shown that Shh-M partially preserved dopaminergic axons around the injection track in the lesioned striatum.

In this study the site of 6-OHDA injection placement was slightly medial, caudal, and ventral to that which we have described previously (43). This led to a more severe depletion of dopaminergic fibers and neurons on the lesioned side [60% remaining dopaminergic cells vs 72% in the previous study (43)] and greater apomorphine-induced rotation. Similar to our previous study, we found that intrastriatal GDNF attenuated the drug-induced rotation and loss of nigral dopaminergic neurons and also resulted in a preservation of TH-IR axons adjacent to the injection site. The preservation of nigral TH-IR neurons was not as great as in our original study despite using the dose of GDNF that was the most effective in our original study (43). This may be due to a somewhat much more severe lesion in the present study or differences in the formulation of GDNF used.

The behavioral and anatomical effects of Shh in the model used in this study revealed some interesting similarities and differences from those of GDNF. There was no difference in the level of attenuation of drug-induced rotation between the group treated with the lowest dose of Shh and the GDNF-treated group. However, there were differences between these groups in the preservation of TH-IR axons around injection sites, the density of TH-IR fibers around a needle track, and the preservation of nigral dopaminergic neurons. In addition, the GDNF-treated group showed locomotor hyperactivity in an open-field activity test in concordance with the previous study (24), while there was no difference between the group treated with Shh at the lowest dose and the vehicle-treated group.

The neural system responsible for the behavioral effects of Shh-M remains to be fully identified. The effect may have simply been due to preservation of dopaminergic axons. Prior studies of GDNF in rat models of PD have shown that functional recovery depends not only on preservation of the nigral cell bodies, but more critically on the ability of the reagent to promote significant reinnervation of the denervated striatum (23, 39, 52). Indeed, Shh-M at the lowest dose partially preserved TH-IR fibers around the injection site. However, the GDNF-treated group and the group treated with 180 ng Shh-M had similar levels of attenuation of apomorphine- and amphetamine-induced rotation, but the area and density of preserved TH-IR fibers in the group treated with 180 ng of Shh-M were considerably

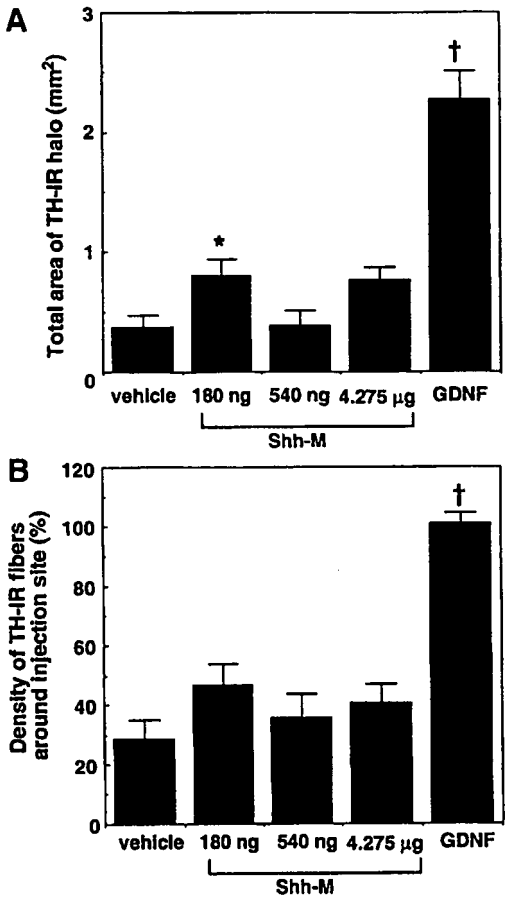

FIG. 5. (A) Total area of the TH-IR halo. (B) Density of TH-IR fibers around the injection site. Twelve measurements were taken in each brain and averaged. Values are means ± SEM. *Significantly different from vehicle and 540 ng Shh-M, $P < 0.05$. †Significantly different from vehicle and the three doses of Shh-M, $P < 0.01$.

smaller than that in GDNF-treated group. The observed difference may be simply due to differences in the sensitivity of the assay between behavioral and immunocytochemical markers; e.g., two levels of preservation of dopaminergic innervation of the striatum may result in similar rotational behavior. This disparity between the behavior and the anatomical indices suggests that factors other than preservation of dopaminergic axons play a significant role.

Another possibility could be that the rotational effect of Shh could have been due to the preservation of dopaminergic fibers coupled with an increase in production of dopamine in the remaining fibers. Such effects have been noted in GDNF and related trophic factors (19, 23, 24). Since our study was designed to evaluate the behavioral and anatomical effects of Shh and the animals were perfused, we were not able to measure the levels of dopamine and its metabolites in this study. Further studies will be needed to elucidate the mechanism for the effects observed with Shh.

A third possibility is conceivable that the nondopaminergic system, e.g., the intrinsic striatal GABAergic neurons, is also involved in the reduction of drug-induced rotational behavior (3, 30). Shh is known to promote the survival of GABAergic neurons in addition to supporting the survival of dopaminergic cells in the midbrain cultures (31). Furthermore, Engber *et al.* (personal communication) recently showed that a single intrastriatal injection of Shh-M 48 h before the excitotoxin malonate caused a dose-dependent reduction in lesion volume. Therefore, the effect of Shh on striatal GABAergic neurons may be significant. Finally, investigators have also shown that the integrity of one neurotransmitter system in the striatum may affect injury to another striatal system (27). As the full role of Shh in the nigrostriatal system is incompletely understood, the possibility exists that Shh may have

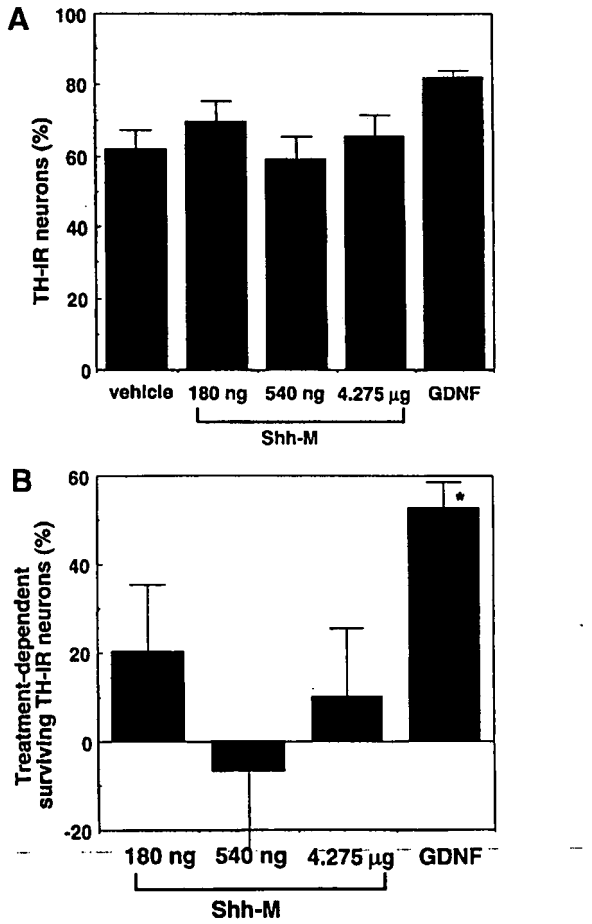

FIG. 6. (A) The number of TH-IR neurons in the SNpc ipsilateral to the injection site was expressed as a percentage of the number in the SNpc contralateral to the injection site. (B) Percentage of treatment-dependent surviving TH-IR neurons was calculated as [(remaining TH-IR neurons on lesioned side as a percentage of intact side in each animal in treatment group − average remaining TH-IR neurons on lesioned side as a percentage of intact side in the vehicle-treated group)/average loss of TH-IR neurons on lesioned side as a percentage of intact side in the vehicle-treated group] × 100. Values are means ± SEM. *Significant difference from the control ($P < 0.001$, Student's t test).

affected the actions of 6-OHDA or subsequent postlesioning events by indirect actions on the nigostriatal dopaminergic system.

The behavioral effects of Shh-M did not increase with increasing doses of Shh-M, as is typically seen with classical pharmacological agents. This beneficial effect of Shh at a low dose but not higher doses is similar to the effect of NGF on axonal growth from rat dorsal root ganglion neurons (11). Furthermore, in studies in which Shh protected adult rat striatal neurons from the excitotoxic effects of malonate injection, a bell-shaped dose response was observed (12; Engber *et al.*, personal communication).

The pattern that we observed in this study may reflect the fact that Shh typically acts as a gradient morphogen (53) and can have different effects at different concentrations. For example, during development of the ventral neural tube, Shh is secreted by the notochord and floor plate and diffuses into the adjacent neural epithelium. Shh induces differentiation of the responding cells into different neuronal subtypes at different concentration thresholds, and the concentration of the Shh is dependent on the distance from the source of Shh (6). For Shh and other gradient morphogens, such as activin and decapentaplegia, cells may respond to only certain concentrations of the differentiation factor and have a certain response to a low concentration and a different or no response to a higher concentration (17, 25, 53). An excellent example of this phenomenon was recently reported by Agarwala *et al.* (1). When an ectopic source of Shh was created close to the normal Shh source in the chick midbrain at embryonic day 2, the cell types normally occupying arcuate territories most distant from the normal Shh source (and normally exposed to the lowest concentration of Shh) were lost from the center of the pattern. This finding suggests that the level of signal provided by the two nearby Shh sources was too high to specify the arcuate territories that were lost. During development, Shh clearly can have specific effects at certain concentrations and these effects are lost at higher concentrations. Our data suggest that a similar phenomenon may hold true in the striatum of the adult rat, and Shh may cause a certain effect at lower but not higher doses.

The active Shh signal binds to a receptor complex composed of at least two transmembrane proteins, Patched and Smoothened (28, 45). Shh binding to Patched is thought to relieve Patched-mediated inhibition of Smoothened activity, resulting in the activation of transcriptional targets by members of the *Gli* family (32, reviewed in 21). Although the transcripts of the Patched and Smoothened genes are expressed in the striatum (49), the mechanism through which Shh prevented behavioral impairment is not yet fully understood. It is possible that additional proteins are induced by Shh and participate in the prevention of behavioral impairments.

Our results are the first demonstration *in vivo* that intrastriatal administration of Shh-M reduces behavioral impairment induced by intrastriatal 6-OHDA lesion. Previous studies had demonstrated a role for Shh in induction of dopaminergic neurons (20, 50), the promotion of the survival of dopaminergic neurons *in vitro,* and the protection of midbrain dopaminergic neurons from the toxic insult of MPP^+ *in vitro* (31). The effective dose of Shh-M caused a reduction in apomorphine- and amphetamine-induced rotation similar to that caused by GDNF despite less preservation of dopaminergic fibers. This observation suggests that Shh may affect the extrapyramidal system by mechanisms other than action on the nigral dopaminergic neurons. This study revealed a novel function of a multifaceted protein and lays the foundation for the use of Shh in new therapeutic approaches for disorders that affect the nigrostriatal system, such as PD.

ACKNOWLEDGMENTS

We thank Drs. Tom Engber and Alphonse Galdes of Biogen for providing Shh-M and helpful discussions of the study. We also thank T. A. Kimber and Q. W. Heinemann for their technical support. This research was supported by Biogen.

REFERENCES

1. Agarwala, S., T. A. Sanders, and C. W. Ragsdale. 2001. Sonic hedgehog control of size and shape in midbrain pattern formation. *Science* **291**: 2147–2150.
2. Ahlgren S. C., and M. Bronner-Fraser. 1999. Inhibition of Sonic hedgehog signaling *in vivo* results in craniofacial neural crest cell death. *Curr. Biol.* **9**: 1304–1314.
3. Araujo, D. M., and D. C. Hilt. 1997. Glial cell line-derived neurotrophic factor attenuates the excitotoxin-induced behavioral and neurochemical deficits in a rodent model of Huntington's disease. *Neuroscience* **81**: 1099–1110.
4. Bilang-Bleuel, A., F. Revah, P. Colin, I. Locquet, J.-J. Robert, J. Mallet, and P. Horellou. 1997. Intrastriatal injection of an adenoviral vector expressing glial-cell-line-derived neurotrophic factor prevents dopaminergic neuron degeneration and behavioral impairment in a rat model of Parkinson disease. *Proc. Natl. Acad. Sci. USA* **94**: 8818–8823.
5. Björklund, A., C. Rosenblad, C. Winkler, and D. Kirik. 1997. Studies on neuroprotective and regenerative effects of GDNF in a partial lesion model of Parkinson's disease. *Neurobiol. Dis.* **4**: 186–200.
6. Briscoe, J., and J. Ericson. 1999. The specification of neuronal identity by graded sonic hedgehog signalling. *Semin. Cell. Dev. Biol.* **10**: 353–362.
7. Bumcrot, D., R. Takada, and A. P. McMahon. 1995. Proteolytic processing yields two secreted forms of Sonic hedgehog. *Mol. Cell. Biol.* **15**: 2294–2303.
8. Carman, L. S., F. H. Gage, and C. W. Shults. 1991. Partial lesion of the substantia nigra: Relation between extent of lesion and rotational behavior. *Brain Res.* **553**: 275–283.
9. Chiang, C., Y. Litingtung, E. Lee, K. E. Young, J. L. Corden, H. Westphal, and P. A. Beachy. 1996. Cyclopia and defective axial

patterning in mice lacking *Sonic hedgehog* gene function. *Nature* **383:** 407–413.

10. Choi-Lundberg, D. L., Q. Lin, Y. N. Chang, Y. L. Chiang, C. M. Hay, H. Mohajeri, B. L. Davidson, and M. C. Bohn. 1997. Dopaminergic neurons protected from degeneration by GDNF gene therapy. *Science* **275:** 838–841.
11. Conti, A. M., S. J. Fischer, and A. J. Windebank. 1997. Inhibition of axonal growth from sensory neurons by excess nerve growth factor. *Ann. Neurol.* **42:** 838–846.
12. Engber, T. M., S. Wang, C. Huang, J. Reilly, A. Galdes, and N. Mahanthappa. 1999. Sonic hedgehog is neuroprotective in the adult striatum in vivo. *Soc. Neurosci. Abstr.* **25:** 1534.
13. Ericson, J., J. Muhr, M. Placzek, T. Lints, T. M. Jessell, and T. Edlund. 1995. Sonic hedgehog induces the differentiation of ventral forebrain neurons: A common signal for ventral patterning within the neural tube. *Cell* **81:** 747–756.
14. Fietz, M. J., J.-P. Concordet, R. Barbosa, R. Johnson, S. Krauss, A. P. McMahon, C. Tabin, and P. W. Ingham. 1994. The *hedgehog* gene family in *Drosophila* and vertebrate development. *Development* **120:** 43–51.
15. Gash, D. M., Z. Zhang, and G. Gerhardt. 1998. Neuroprotective and neurorestorative properties of GDNF. *Ann. Neurol. Suppl.* **44:** S121–S125.
16. Gibb, W. R. G. 1992. Neuropathology of Parkinson's disease and related syndromes. *Neurol. Clin.* **10:** 361–376.
17. Gurdon, J. B., P. Harger, A. Mitchell, and P. Lemaire. 1994. Activin signalling and response to a morphogen gradient. *Nature* **371:** 477–478.
18. Hammerschmidt, M., A. Brook, and A. P. McMahon. 1997. The world according to *hedgehog*. *Trends Genet.* **13:** 14–21.
19. Horger, B. A., M. C. Nishimura, M. P. Armanini, L.-C. Wang, K. T. Poulsen, C. Rosenblad, D. Kirik, B. Moffat, L. Simmons, E. Johnson Jr., J. Milbrandt, A. Rosenthal, A. Bjorklund, R. A. Vandlen, M. A. Hynes, and H. S. Phillips. 1998. Neuturin exerts potent actions on survival and function of midbrain dopaminergic neurons. *J. Neurosci.* **18:** 4929–4937.
20. Hynes, M. A., J. A. Porter, C. Chiang, D. Chang, M. Tessier-Lavigne, P. A. Beachy, and A. Rosenthal. 1995. Induction of midbrain dopaminergic neurons by Sonic hedgehog. *Neuron* **15:** 35–44.
21. Ingham, P. W. 1998. Transducing hedgehog: The story so far. *EMBO J.* **17:** 3505–3511.
22. Kirik, D., C. Rosenblad, and A. Björklund. 1998. Characterization of behavioral and neurodegenerative changes following partial lesions of the nigrostriatal dopamine system induced by intrastriatal 6-hydroxydopamine in the rat. *Exp. Neurol.* **152:** 259–277.
23. Kirik, D., C. Rosenblad, A. Björklund, and R. J. Mandel. 2000. Long-term rAAV-mediated gene transfer of GDNF in the rat Parkinson's model: Intrastriatal but not intranigral transduction promotes functional regeneration in the lesioned nigrostriatal system. *J. Neurosci.* **20:** 4686–4700.
24. Lapchak, P. A., P. J. Miller, and S. Jiao. 1997. Glial cell line-derived neurotrophic factor induces the dopaminergic and cholinergic phenotype and increases locomotor activity in aged Fischer 344 rats. *Neuroscience* **77:** 745–752.
25. Lecuit, T., and S. M. Cohen. 1998. Dpp receptor levels contribute to shaping the Dpp morphogen gradient in the *Drosophila* wing imaginal disc. *Development* **125:** 4901–4907.
26. Mandel, R. J., S. K. Spratt, R. O. Snyder, and S. E. Leff. 1997. Midbrain injection of recombinant adeno-associated virus encoding rat glial cell line-derived neurotrophic factor protects nigral neurons in a progressive 6-hydroxydopamine-induced degeneration model of Parkinson's disease in rats. *Proc. Natl. Acad. Sci. USA* **94:** 14083–14088.
27. Maragos, W. F., R. J. Jakel, Z. Pang, and J. W. Geddes. 1998. 6-Hydroxydopamine injections into the nigrostriatal pathway attenuate striatal malonate and 3-nitropropionic acid lesions. *Exp. Neurol.* **154:** 637–644.
28. Marigo, V., R. A. Davey, Y. Zuo, J. M. Cunningham, and C. J. Tabin. 1996. Biochemical evidence that Patched is the Hedgehog receptor. *Nature* **384:** 176–179.
29. Martí, E., D. A. Bumcrot, R. Takada, and A. P. McMahon. 1995. Requirement of 19K of Sonic hedgehog for induction of distinct ventral cell types in CNS explants. *Nature* **375:** 322–325.
30. McKenzie, J. S., D. A. Shafton, and C. A. Stewart. 1991. Intrastriatal dopaminergic agents, muscarinic stimulation, and GABA antagonism compared for rotation responses in rats. *Behav. Brain Res.* **45:** 163–170.
31. Miao, N., M. Wang, J. A. Ott, J. S. D'Alessandro, T. M. Woolf, D. A. Bumcrot, N. K. Mahanthappa, and K. Pang. 1997. Sonic hedgehog promotes the survival of specific CNS neuron populations and protects these cells from toxic insult in vitro. *J. Neurosci.* **17:** 5891–5899.
32. Murone, M., A. Rosenthal, and F. de Sauvage. 1999. Sonic hedgehog signaling by the patched–smoothened receptor complex. *Curr. Biol* **9:** 76–84.
33. Olsson, M., G. Nikkhah, C. Bentlage, and A. Björklund. 1995. Forelimb akinesia in the rat Parkinson model: Differential effects of Parkinson model: Differential effects of dopamine agonists and nigral transplants as assessed by a new stepping test. *J. Neurosci.* **15:** 3863–3875.
34. Paxinos, G., and C. Watson. 1986. *The Rat Brain in Stereotaxic Coordinates*. Academic Press, San Diego, CA.
35. Pepinsky, R. B., C. Zeng, D. Wen, P. Rayhorn, D. P. Baker, K. P. Williams, S. A. Bixler, C. M. Ambrose, E. A. Garber, K. Miatkowski, F. R. Taylor, E. A. Wang, and A. Galdes. 1998. Identification of palmitic acid-modified form of human Sonic Hedgehog. *J. Biol. Chem.* **273:** 14037–14045.
36. Perrimon, N. 1995. Hedgehog and beyond. *Cell* **80:** 517–520.
37. Roelink, H., A. Augusberger, J. Heemskerk, V. Korzh, S. Norlin, A. Ruiz i Altaba, Y. Tanabe, M. Placzek, T. Edlund, T. M. Jessel, and J. Dodd. 1994. Floor plate and motor neuron induction by *vhh-1*, a vertebrate homologue of *hedgehog* expressed by the notochord. *Cell* **76:** 761–775.
38. Rosenblad, C., A. Martinez-Serrano, and A. Björklund. 1996. Glial cell line-derived neurotrophic factor increases survival, growth and function of intrastriatal fetal nigral dopaminergic grafts. *Neuroscience* **75:** 979–985.
39. Rosenblad, C., D. Kirik, and A. Björklund. 2000. Sequential administration of GDNF into the substantia nigra and striatum promotes dopamine neuron survival and axonal sprouting but not striatal reinnervation or functional recovery in the partial 6-OHDA lesion model. *Exp. Neurol.* **161:** 503–516.
40. Sauer, H., C. Rosenblad, and A. Björklund. 1995. Glial cell line-derived neurotrophic factor but not transforming growth factor β3 prevents delayed degeneration of nigral dopaminergic neurons following striatal 6-hydroxydopamine lesion. *Proc. Natl. Acad. Sci. USA* **92:** 8935–8939.
41. Schierle, G. S., O. Hansson, M. Leist, P. Nicotera, H. Winder, and P. Brundin. 1999. Caspase inhibition reduces apoptosis and increases survival of nigral transplants. *Nat. Med.* **5:** 97–100.
42. Shults, C. W., T. Kimber, and C. A. Altar. 1995. BDNF attenuates the effects of intrastriatal injection of 6-hydroxydopamine. *NeuroReport* **6:** 1109–1112.
43. Shults, C. W., T. Kimber, and D. Martin. 1996. Intrastriatal injection of GDNF attenuates the effects of 6-hydroxydopamine. *NeuroReport* **7:** 627–631.

44. Smith, J. C. 1994. Hedgehog, the floor plate, and the zone of polarizing activity. *Cell* **76**: 193–196.

45. Stone, D. H., M. Hynes, M. Armanini, T. A. Swanson, Q. Gu, R. L. Johnson, M. P. Scott, D. Pennica, A. Goddard, H. Phillips, M. Noll, J. E. Hooper, F. de Sauvage, and A. Rosenthal. 1996. The tumor-suppressor gene *patched* encodes a candidate receptor for Sonic hedgehog. *Nature* **384**: 129–134.

46. Studer, L., V. Tabar, and R. D. G. McKay. 1998. Transplantation of expanded mesencephalic precursors leads to recovery in parkinsonian rats. *Nat. Neurosci.* **1**: 290–294.

47. Tanabe, Y., H. Roelink, and T. M. Jessell. 1995. Induction of motor neurons by Sonic hedgehog is independent of floor plate. *Curr. Biol.* **5**: 651–658.

48. Taylor, F. R., D. Wen, E. A. Berber, A. N. Camillo, D. P. Baker, R. M. Arduini, K. P. Williams, P. H. Weinreb, P. Rayhorn, X. Hronowski, A. Whitty, E. S. Day, A. Boriack-Sjodin, R. I. Shapiro, A. Galdes, and R. B. Pepinsky. 2001. Enhanced potency of human Sonic hedgehog by hydrophobic modification. *Biochemistry* **40**: 4359–4371.

49. Traiffort, E., D. A. Charytoniuk, H. Faure, and M. Ruat. 1998. Regional distribution of Sonic Hedgehog, Patched, and Smoothened mRNA in the adult rat brain. *J. Neurochem.* **70**: 1327–1330.

50. Wang, M. Z., P. Jin, D. A. Bumcrot, V. Marigo, A. P. McMahon, E. A. Wang, T. Woolf, and K. Pang. 1995. Induction of dopaminergic neuron phenotype in the midbrain by Sonic hedgehog protein. *Nat. Med.* **1**: 1184–1188.

51. Williams, K. P., P. Rayhorn, C. Chi-Rosso, E. A. Garber, K. L. Strauch, G. S. B. Horan, J. O. Reilly, D. P. Baker, F. R. Taylor, V. Koteliansky, and R. B. Pepinsky. 1999. Functional antagonists of sonic hedgehog reveal the importance of the N terminus for activity. *J. Cell Sci.* **112**: 4405–4414.

52. Winkler, C., H. Sauer, C. S. Lee, and A. Björklund. 1996. Short-term GDNF treatment provides long-term rescue of lesioned nigral dopaminergic neurons in a rat model of Parkinson's disease. *J. Neurosci.* **16**: 7206–7215.

53. Wolpert, L. 1996. One hundred years of positional information. *Trends Genet.* **12**: 359–364.

Development 120, 3339-3353 (1994)
Printed in Great Britain © The Company of Biologists Limited 1994

Products, genetic linkage and limb patterning activity of a murine *hedgehog* gene

David T. Chang[1], Alric López[2], Doris P. von Kessler[1], Chin Chiang[1], B. Kay Simandl[2], Renbin Zhao[1], Michael F. Seldin[3], John F. Fallon[2] and Philip A. Beachy[1]

[1]Howard Hughes Medical Institute, Department of Molecular Biology and Genetics, The Johns Hopkins School of Medicine, Baltimore, Maryland 21205, USA
[2]Department of Anatomy, Neuroscience Training Program, University of Wisconsin, Madison, Wisconsin 53706, USA
[3]Departments of Medicine and Microbiology, Duke University Medical Center, Durham, North Carolina 27710, USA

SUMMARY

The *hedgehog* (*hh*) segmentation gene of *Drosophila melanogaster* encodes a secreted signaling protein that functions in the patterning of larval and adult structures. Using low stringency hybridization and degenerate PCR primers, we have isolated complete or partial *hh*-like sequences from a range of invertebrate species including other insects, leech and sea urchin. We have also isolated three mouse and two human DNA fragments encoding distinct *hh*-like sequences. Our studies have focused upon *Hhg-1*, a mouse gene encoding a protein with 46% amino acid identity to *hh*. The *Hhg-1* gene, which corresponds to the previously described vhh-1 or sonic class, is expressed in the notochord, ventral neural tube, lung bud, hindgut and posterior margin of the limb bud in developing mouse embryos. By segregation analysis the *Hhg-1* gene has been localized to a region in proximal chromosome 5, where two mutations affecting mouse limb development previously have been mapped. In *Drosophila* embryos, ubiquitous expression of the *Hhg-1* gene yields effects upon gene expression and cuticle pattern similar to those observed for the *Drosophila hh* gene. We also find that cultured quail cells transfected with a *Hhg-1* expression construct can induce digit duplications when grafted to anterior or mid-distal but not posterior borders within the developing chick limb; more proximal limb element duplications are induced exclusively by mid-distal grafts. Both in transgenic *Drosophila* embryos and in transfected quail cells, the *Hhg-1* protein product is cleaved to yield two stable fragments from a single larger precursor. The significance of *Hhg-1* genetic linkage, patterning activity and proteolytic processing in *Drosophila* and chick embryos is discussed.

Key words: mouse, *hedgehog*, genetic linkage, limb development, gene expression, *Hammertoe*, *Hemimelic extra toes*

INTRODUCTION

Experimental manipulations of vertebrate embryos have revealed the existence of organizing centers that appear to function in the patterning of adjacent structures. The dorsal blastopore lip in *Xenopus*, for example, appears to control development of the major body axis (Spemann, 1933), while the posterior margin of the limb bud or ZPA (zone of polarizing activity or polarizing region) is capable of imposing pattern upon developing limbs (Saunders and Gasseling, 1968; Wolpert, 1969). Because these and other organizing centers contribute few of the cells that constitute the actual structure being formed, patterning activity is inferred to occur through the agency of molecules secreted from the organizing center. Until recently, however, little was known about the nature and identity of these molecules.

Drosophila development has long served as a model system for the study of molecules important in vertebrate developmental processes, including secreted signaling proteins. For example, the product of the *dpp* (*decapentaplegic*) gene, a member of the TGF-β super-family of signaling molecules which is expressed at the dorsal pole of the embryo, acts as a concentration-dependent factor capable of imposing pattern along the entire dorsal-ventral axis of the embryo (Ferguson and Anderson, 1992). The *wingless* (*wg*) segment polarity gene, a member of the *Wnt* super-family that also includes many vertebrate representatives (reviewed by Nusse and Varmus, 1992), encodes another signaling protein that acts at somewhat shorter range in segmentation and in patterning of the embryonic cuticle. Early expression of the *wg* gene in a stripe of cells bordering the parasegment boundary is required for maintenance of appropriate gene expression in an adjacent stripe of cells on the opposite side of the parasegment boundary (DiNardo et al., 1988; Martinez Arias et al., 1988); at a later stage, specification of appropriate differentiated fates depends upon expression of the *wg* product in neighboring cells (Baker, 1988; Bejsovec and Martinez-Arias, 1991; Dougan and DiNardo, 1992).

Another *Drosophila* segment polarity gene that has been implicated as encoding a signaling molecule with an important role in patterning is *hedgehog* (*hh*). Clones of mutant cells lacking *hh* function appear to affect adjacent structures in the

eye and cuticle of the *Drosophila* adult (Mohler, 1988; Heberlein et al., 1993; Ma et al., 1993). In the embryo, *hh* transcription is restricted to cells in a narrow stripe adjacent to and non-overlapping with the *wingless* stripe; *hh* mutations, however, affect gene expression and cuticle pattern elements in cells outside this zone of transcription (Mohler and Vani, 1992; Lee et al., 1992; Tabata et al., 1992; Tashiro et al., 1993). The notion that *hedgehog* encodes a secreted signaling molecule is also supported by other types of evidence – in vitro translated protein products can be secreted into microsomes (Lee et al., 1992) and immunostaining of *Drosophila* embryos shows that the *hh* protein is distributed in stripes that are broader than the stripes of *hh* transcription (Taylor et al., 1993; Tabata and Kornberg, 1994; von Kessler, D.V. and Beachy, P.A. unpublished observations). Molecular characterization of the *Drosophila hh* gene (Lee et al., 1992; Mohler and Vani, 1992; Tabata et al., 1992; Tashiro et al., 1993) revealed no sequence similarities to the products of other genes, despite the fact that many segment polarity genes do have homologues in other species (see Peifer and Bejsovec, 1992 for a review). More recently, however, several groups have demonstrated the existence of *hedgehog* homologs in chick, mouse, zebrafish and rat (Echelard et al., 1993; Krauss et al., 1993; Riddle et al., 1993; Roelink et al., 1994; S. C. Ekker and P. A. B., unpublished data).

Here we present evidence for broad evolutionary conservation of *hedgehog* sequences among invertebrate species. We also confirm the existence of a family of at least three mouse *hedgehog* homologues (Echelard et al., 1993) and demonstrate the existence of two new human *hedgehog* homologues. We show that *Hhg-1*, the mouse homologue which corresponds to the independently identified vhh-1 and sonic *hedgehog* genes in the rat and the mouse (Roelink et al., 1994; Echelard et al., 1993), is expressed in the notochord, ventral neural tube, lung bud, hindgut and posterior limb bud margin in developing mouse embryos. To elucidate *Hhg-1* function, we first demonstrated that *Hhg-1* yields effects upon gene expression and cuticle pattern similar to those of the *Drosophila hh* gene when ubiquitously expressed in *Drosophila* embryos. We also found that grafts of cells expressing *Hhg-1* can impose pattern upon the developing chick limb. In both of these systems, the *Hhg-1* protein product is cleaved to yield two stable fragments from a single larger precursor. Consistent with a role in limb patterning, we mapped *Hhg-1* by segregation analysis to a region of mouse chromosome five with tight linkage to two previously mapped limb mutants. Proteolytic processing of *Hhg-1* products and their ability to function in *Drosophila* embryos as well as in vertebrate limb patterning suggests widespread conservation of the fundamental mechanisms underlying function of the *hedgehog* multi-gene family.

MATERIALS AND METHODS

Isolation of *hedgehog* homologues

Genomic clones from *Drosophila hydei* and the mosquito *Anopheles gambiae* were isolated by low-stringency screening (hybridization at 52°C, 6× SSC; washes in 2× SSC) of a *D. hydei* genomic library in the EMBL4 lambda phage vector (a gift of M. Claudia and D. Sullivan) and of an *A. gambiae* genomic library in the lambda phage vector DASH 2 (kindly provided by J. Kassis). The initial probe for this screen corresponded to positions 389-1801 (numbering according to Lee et al., 1992), and further analysis of the *D. hydei* clone using exon-specific probes identified three hybridizing regions that corresponded to exons 1, 2 and 3 of *D. melanogaster hh*. The flour beetle (*Tribolium castaneum*; DNA a gift from Sue Brown), the leech (*Hirudo medicinalis*; DNA a gift from G. Aisemberg), the sea urchin (*Strongylocentrotus purpuratus*; DNA a gift from A. Cameron) and the mouse and human *hh*-like sequences were initially isolated by polymerase chain reaction (PCR) using primers degenerate for all possible coding combinations of the sequences underlined in Fig. 1. PCR amplifications contained from 100 ng to 2 μg genomic DNA (depending upon the genome size of the species), 2 μM of each primer, 200 μM dNTPs (Pharmacia), 1× reaction buffer (Boehringer-Mannheim) and 2.5 units Taq polymerase (Boehringer-Mannheim) in 50 μl reactions. Amplification was as follows: 94°C 5 minutes, addition of Taq polymerase at 75°C, followed by 94°C 1 minute, 52°C 1.5 minutes and 72°C 1 minute for 30 cycles and a final extension of 72°C for 5 minutes. All PCR products were cloned into pBluescript (Stratagene) prior to sequence determination. No *hh*-like sequences were obtained using DNA from *Dictyostelium* or from *C. elegans* using this approach.

Mouse clones obtained in this manner contained 144 bases of sequence between the primer ends and were labelled with [α-^{32}P]dATP and used for high stringency screens of mouse cDNA libraries made from whole 8.5 dpc embryonic RNA (Lee, 1990) and from 14.5 dpc embryonic brain in the λZAP vector (a gift from A. Lanahan). Several clones corresponding to *Hhg-1* were isolated and the largest, 2629 bp in length (pDTC8.0), was chosen for sequence analysis using dideoxy chain termination (Sanger et al., 1977) and Sequenase v2.0 (US Biochemicals). Compressions were resolved by using 7-deaza guanosine (US Biochemicals). Sequence analysis made use of the Geneworks 2.0 (IntelliGenetics) and MacVector 3.5 (IBI) software packages.

Analysis of RNA expression in mouse and *Drosophila* embryos

For northern blot analysis, RNA from mouse embryos and from mouse adult tissues was isolated, electrophoresed in 1.2% agarose, blotted and probed, essentially as described by Ausubel et al. (1993). The probe used was made by random hexamer primed synthesis using the pDTC8.0 insert as a template in the presence of [α-^{32}P]dATP. Hybridizations and washes were performed under standard high stringency conditions (Ausubel et al., 1993).

In situ hybridization to sections of mouse embryos was essentially as described Wilkinson (1992), except that [α-^{33}P]rUTP was substituted in place of [α-^{35}S]rUTP for riboprobe synthesis. Briefly, 7.5-10.5 dpc mouse embryos were harvested, fixed in ice-cold 4% paraformaldehyde in PBS, dehydrated through an ethanol series, cleared in xylene and embedded in paraffin. 6 μm sections were floated on a 48°C water bath, transferred to AAS (3-aminopropyltriethoxysilane, Sigma) subbed slides, dewaxed with xylene and hybridized overnight to riboprobe in the sense or antisense orientations. Slides were washed under high-stringency conditions, dipped in Kodak NTB-2 emulsion and developed after a 10 day exposure. All sections were then stained for 30 seconds with haematoxylin (Polysciences) and mounted with Permount (Fisher). Sense and antisense probes were synthesized using a riboprobe synthesis kit from Stratagene with a 249 bp *Bam*HI/*Sma*I fragment of pDTC8.0 that extends from residues 297 to 380 within the *Hhg-1* open reading frame (Fig. 1) subcloned into Bluescript as template (pDTC1.8). Adobe Photoshop was used for superimposition of bright-field and dark-field views, collected in digital form using a Sony 3 CCD camera attached to a Zeiss Axioplan microscope and transferred directly to a Macintosh Quadra 800 equipped with a Nuvista Video Capture Board.

In situ hybridization to *Drosophila* embryos was performed according to standard methods (Tautz and Pfeifle, 1989). The *wingless* (*wg*) probe was made by random hexamer primed synthesis (Feinberg and Vogelstein, 1983) using a 2.2 kb *Hin*dIII/*Xba*I fragment from a

wg cDNA (gift from R. Nusse; Rijsewijk et al., 1987) as template. Probe synthesis was carried out in the presence of digoxigenin-dUTP (Boehringer Mannheim).

Drosophila germ-line transformation and phenotypic analysis

The hs*hh* construct was made by inserting a blunted 1581 bp *MseI* fragment containing the full *hh* ORF (from 327 to 1908, Lee et al., 1992) into the *StuI* site of pCaSpeR-hs (Thummel et al., 1988; from C. Thummel, University of Utah, Salt Lake City). The hs*Hhg-1* construct was made by inserting a blunted 1330 bp *Bsu*36I/*Eco*57I fragment from pDTC8.0 that contained the entire *Hhg-1* open reading frame into the *StuI* site of pCaSpeR-hs. hs*hh* and hs*Hhg-1* each were coinjected with pπ25.2 wc into w^{1118} embryos using a standard protocol for P element-mediated transformation (Rubin and Spradling, 1982). Germ line transformants with P element integration on the third chromosome were isolated for each construct; hs*hh* was maintained as a homozygous stock and hs*Hhg-1* was maintained over the TM3 balancer chromosome.

Embryos for cuticle analysis were collected and aged at 25°C and heat shocked for 1 hour at 37°C. After further incubation for 24 hours at 25°C, embryos were dechorionated, transferred to Hoyer's mountant (Wieschaus and Nusslein-Volhard, 1986) and incubated at 65°C for 5 hours. For in situ hybridization, *Drosophila* embryos from the hs-*hh*, hs-*Hhg-1* and w^{1118} parent lines were collected for 5 hours at 25°C, aged an additional 5 hours at 25°C, heat shocked for 1 hour at 37°C and allowed to recover at 25°C for an additional hour before fixation.

Chick limb patterning assays

Isolation and characterization of the quail cell line QT6 has been described (Moscovici et al., 1977). QT6 cells were cultured on 3.5 cm uncoated plastic culture dishes (Falcon) in growth medium (M199 medium plus Earles balanced salt solution [Gibco, Grand Island, NY] supplemented with 10% tryptose phosphate broth, 5% fetal calf serum, 1% dimethylsulfoxide, 100 U/ml of penicillin and 100 μg/ml of streptomycin) in a 5% CO_2 atmosphere.

QT6 cells were transiently transfected by a modified calcium phosphate method (Chen and Okayama, 1987). In brief, after preincubation in transfection medium (DMEM plus 5% fetal calf serum + 1% DMSO) 20-25μg of precipitated DNA was added to 70-80% confluent QT6 cells in dishes. After overnight incubation, the DNA precipitate was removed and complete growth medium added. The pCIS plasmid, which carries a cytomegalovirus (CMV) promoter and SV40 intron and polyadenylation signal (Gorman, 1985), was used as the expression vector. Expression constructs included pCIS*lacZ* and pCIS*Hhg-1*, which contain *lacZ* and *Hhg-1* respectively under control of the CMV promoter. To assess transfection efficiency parallel plates were transfected with equimolar amounts of either pCIS-*lacZ* or pCIS*Hhg-1*.

For β-galactosidase activity staining, cells and limb buds were fixed 5 minutes and 1 hour, respectively, in PBS containing 2% formaldehyde and 0.2% glutaraldehyde. After rinsing in PBS, samples were incubated in X-gal cocktail (1 mg/ml X-gal (5-bromo-4-chloro-3-indolyl b-D-galactopyranoside), 2 mM $MgCl_2$, 16 mM $K_3Fe(CN)_6$, 16 mM $K_4Fe(CN)_6$) for 18-24 hours at 22°C.

Transiently transfected QT6 cells were scraped from tissue culture plates with a Teflon scraper (Falcon) and dissociated by repeated pipetting. Poly-D-lysine (Sigma, P1149) was added to the cell suspension to a concentration of 33 μg/ml. Cells were then pelleted by centrifugation at 1×10^3 revs/minute on a benchtop microfuge for 10 seconds. Wedge-shaped fragments were excised from the pelleted cells and grafted to anterior, mid-distal, or posterior slits made with fine forceps in stage 20-21 chick wing buds (Riley et al., 1993). Embryos harvested at day 10 were fixed overnight in 10% formaldehyde, stained with Victoria blue and cleared in methyl salicylate (see Riley et al., 1993).

Detection of *Hhg-1* protein

Region-specific antibodies were generated by immunization of New Zealand White rabbits with PCR-generated, His_6-tagged fusions (in the vector pTrcHis from InVitrogen, San Diego, CA) to residues 25-159 (N-terminal) and 202-389 (C-terminal) of the *Hhg-1* ORF (Fig. 1). Following repeated boosts, reactive sera were purified using affinity matrices carrying fusions of glutathione-S-transferase to the same portions of the *Hhg-1* ORF (in the vector pGEX from Amrad, Melbourne, Australia). Specific antibodies were eluted with a buffer containing 100 mM glycine-HCl at pH 2.5 (Harlow and Lane, 1988).

For immunodetection, samples of tranfected and untransfected QT6 cells and of heat-shocked wild-type and hs*Hhg-1* Drosophila embryos were suspended and boiled in sample loading buffer and electrophoresed in 12% polyacrylamide-SDS gels (Laemmli, 1970). Following transfer to nitrocellulose (Burnette, 1981), proteins were detected by chemiluminescence (with the ECL kit from Amersham), with affinity purified anti-*Hhg-1* antibodies at a dilution of 1/300 and HRP-conjugated goat anti-rabbit 2° antibody (Jackson ImmunoResearch, Baltimore MD) at a dilution of 1/10,000.

Chromosome localization of *Hhg-1*

C3H/HeJ-*gld* and *Mus spretus* (Spain) mice and [(C3H/HeJ-*gld* × Mus spretus)F_1 × C3H/HeJ-*gld*] interspecific backcross mice were bred and maintained as previously described (Seldin et al., 1988) *Mus spretus* was chosen as the second parent in this cross because of the relative ease of detection of informative restriction fragment length variants (RFLV) in comparison with crosses using conventional inbred laboratory strains.

DNA isolated from mouse organs by standard techniques was digested with restriction endonucleases and 10 μg samples were electrophoresed in 0.9% agarose gels. DNA was transferred to Nytran membranes (Schleicher & Schuell, Inc., Keene, NH), hybridized at 65°C and washed under stringent conditions, all as previously described (Sambrook et al., 1989). Clones used as probes in the current study included a ~500 bp 3′-UTR of *Hhg-1*, a quinoid dihydropteridine reductase (Qdpr) clone, DHPR13 (Lockyer et al., 1987) and an interleukin 6, (Il-6) specific clone, 27-4 (Mock et al., 1989).

Gene linkage was determined by segregation analysis (Green, 1981). Gene order was determined by analyzing all haplotypes and minimizing crossover frequency between all genes that were determined to be within a linkage group. This method resulted in determination of the most likely gene order (Bishop, 1985).

Characterization of *Hhg-1* sequences in *Hm* and *Hx* mutants

DNA from heterozygous *Hm* (AKR.C3H-*Ca Hm Sl*) and heterozygous *Hx* (B10.D2/nSn-*Hx*/+) mutant individuals were obtained from Jackson Laboratory and digested with *Eco*RI, *Bam*HI, *Taq*I, *Hin*dIII, *Alu*I, *Rsa*I, *Dpn*I, *Hin*fI and *Hin*pI. These digests were electrophoresed, blotted and probed as above with ^{32}P-labelled pDTC8.0 and compared to similarly digested and probed DNAs from parental strains. No differences in restriction fragment lengths were detected for either mutant. This analysis would have detected differences as small as 100 bp.

Hhg-1 coding sequences were isolated by PCR amplification from genomic DNA of individuals heterozygous for the *Hx* mutation (B10.D2/nSn-*Hx*/+; Jackson Labs). Analysis included eleven independent clones representing coding sequences from exon one, fourteen independent clones representing coding sequences from exon two and eight independent clones representing coding sequences from exon three.

RESULTS

Isolation of *hedgehog* homologues

As a first step toward isolation of *hedgehog* homologues from distant species, we used low-stringency hybridization to isolate

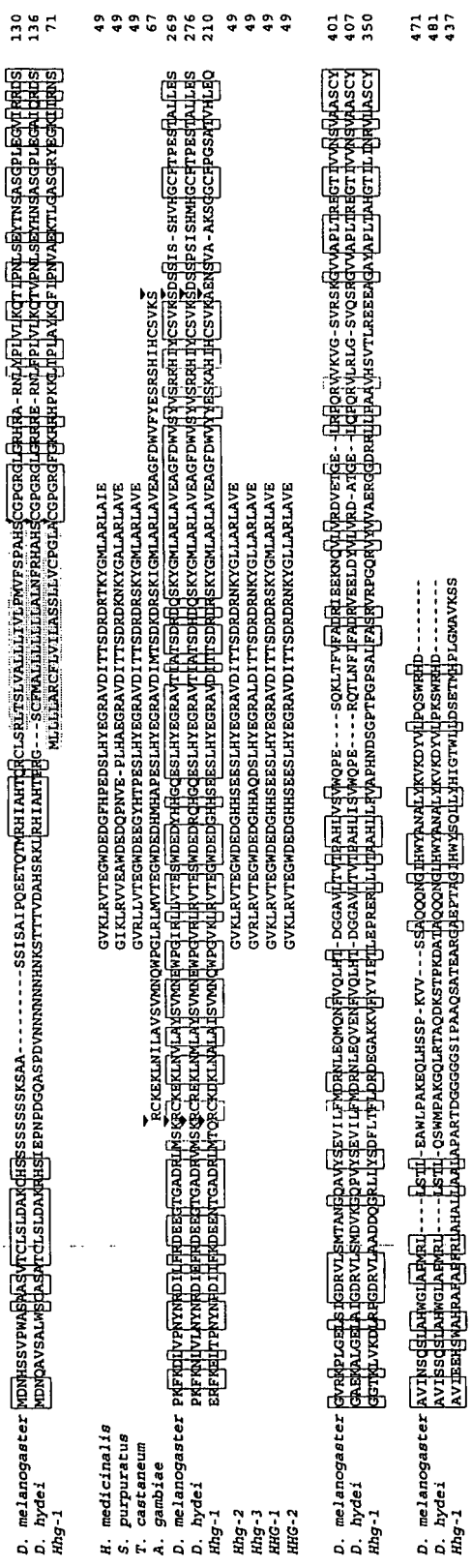

genomic *hh* clones from two other dipterans, *Drosophila hydei* and the mosquito *Anopheles gambiae*. We then used the polymerase chain reaction (PCR) with degenerate primers from conserved regions within the second exon (underlined regions in Fig. 1) to isolate single *hh*-like sequences from genomic DNA of the flour beetle, leech and sea urchin, and multiple sequences from mouse and man. No *hh*-like sequences were obtained using DNA from *Dictyostelium* or from *C. elegans* by this approach. From sequence comparisons, human PCR fragments 1 and 2 appear to correspond most closely to mouse fragments 1 and 2, respectively.

Our focus here is primarily upon one of the three mouse clones, *Hhg-1*, which when used as a probe yielded a 2.0 kb clone from a 8.5 dpc mouse embryonic cDNA library and a 2.7 kb clone from a 14.5 dpc embryonic cDNA library. The 2.7 kb cDNA appears to represent a nearly full-length mRNA because it corresponds to a 2.8 kb band detected by hybridization on a northern blot (see below). The largest methionine-initiated open reading frame within this cDNA encompasses 437 codons and is preceded by one in frame upstream stop codon (not shown). Sequence comparisons indicate that the protein encoded by *Hhg-1* is identical to the independently characterized mouse *Shh* (Echelard et al., 1993) except for an arginine to lysine difference at residue 122. *Hhg-1* also corresponds closely to the rat *vhh-1* gene (97% amino acid identity; Roelink et al., 1994), the chicken *Sonic hedgehog* (81% identity; Riddle et al., 1993) and *Shh* from the zebrafish (68% identity; Krauss et al., 1993; Roelink et al., 1994; S.C. Ekker and P.A.B., unpublished data). The PCR-generated fragments *Hhg-2* and *Hhg-3* appear to correspond to the *Indian* and *Desert* classes of mouse *hedgehog* genes, respectively (Echelard et al., 1993).

Alignment of the *Hhg-1* open reading frame with the two *Drosophila hh* sequences (Fig. 1) shows that all three proteins contain hydrophobic amino acid sequences near their amino-termini; the hydrophobic stretches within the *D. melanogaster* protein (residues 64 to 83) and within the mouse protein are known to act efficiently as signal sequences for cleavage (Lee et al., 1992, and J. J. Lee and P. A. B., unpublished data). Both *Drosophila* signal sequences are unusual in their internal locations, while the hydrophobic stretch of the mouse gene occurs at the extreme amino-terminus, a more conventional location for cleaved signal sequences. Although portions of

Fig. 1. Multiple mammalian and invertebrate *hedgehog*-like sequences. The *Drosophila melanogaster hedgehog* open reading frame is shown aligned with a complete *hedgehog* coding sequence deduced from genomic sequence for *Drosophila hydei* and a complete mouse coding sequence (*Hhg-1*) deduced from a cDNA clone. Amino acid identities between these complete sequences are boxed, Kyte-Dolittle hydrophobic domains are shaded, predicted signal sequence cleavage sites (von Heijne, 1986) are indicated by an arrow; and intron/exon boundaries are marked by triangles. Below these complete sequences are shown partial sequences deduced from cloned PCR products for two other mouse genes (*Hhg-2* and *Hhg-3*) and two human sequences (*HHG-1* and *HHG-2*). Sequences from invertebrate species above the complete sequence alignments include partial sequences for the mosquito *Anopheles gambiae* (from a genomic clone) and PCR-derived sequences from the flour beetle, *Tribolium castaneum*, the urchin, *Strongylocentrotus purpuratus* and the leech, *Hirudo medicinalis*. Degenerate primers used for PCR reactions incorporated sequence from the underlined portion of the *D. melanogaster* sequence.

sequence N-terminal to the *Drosophila* signal sequences are conserved, suggesting a functional role, the mouse mouse gene lacks this region.

The overall level of amino acid identity between *Hhg-1* and *hh* carboxy-terminal to the signal sequences is 46%. A closer examination shows that the amino terminal portion, from residues 25 to 187, displays 69% identity, while remaining residues in the carboxy-terminal portion display a much lower 31% identity. Like *hh*, the *Hhg-1* coding sequence is divided into three exons and the boundaries of these exons are at the same positions within coding sequence as those of the three *Drosophila hh* exons (see Fig. 1). Curiously, the boundary between coding sequences of the second and third exons occurs near the transition from high to low levels of overall sequence conservation. The coincidence of these two boundaries suggests a possible demarcation of functional domains within these proteins. This location within *Hhg-1* coding sequence also coincides approximately with the site of a presumed proteolytic cleavage (see below).

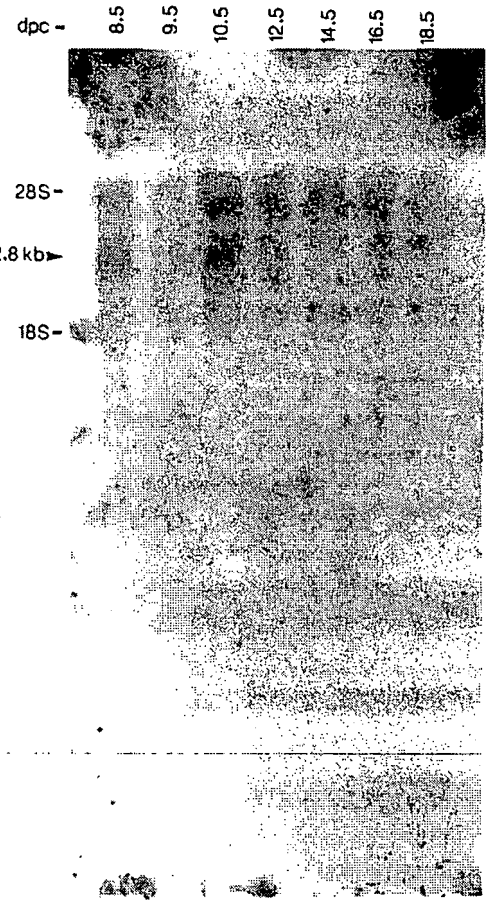

Fig. 2. Electrophoretic analysis of *Hhg-1* RNA. Each lane contains 10 μg total RNA from mouse embryos staged as indicated above the lanes (dpc, days post coitum). The probe, made from the full length *Hhg-1* cDNA, detected a ~2.8 kb band (indicated by arrowhead) in RNA from all stages of embryos examined. The upper band comigrates with the 28S RNA and is due to non-specific hybridization.

Expression of *Hhg-1* in mouse embryos

We began our analysis of *Hhg-1* expression by hybridization of a ^{32}P-labelled *Hhg-1* probe to a northern blot of RNA isolated from embryos ranging from 8.5 to 18.5 dpc. A band of ~2.8 kb was detected at each stage, with a peak at day 10.5 (Fig. 2). These results are similar to those reported by Echelard et al. (1993) for *Shh* except that we detect the 2.8 kb RNA throughout embryogenesis. To obtain more detailed spatial and temporal information regarding *Hhg-1* expression, sections from 7.5, 8.5, 9.5 and 10.5 dpc embryos were hybridized to a ^{33}P-labelled antisense RNA probe under stringent hybridization and wash conditions (see Materials and methods); the corresponding sense RNA probe was used as a control. Selected sections from these in situ hybridizations are presented in Figs 3-5 and described below.

In the 7.5 dpc embryo, *Hhg-1* expression is confined to anterior midline mesoderm. No expression is seen in the overlying ectoderm (Fig. 3B,C) or in other embryonic or extraembryonic tissue (data not shown). Transverse sections confirm restriction of expression in the early gastrula to axial mesoderm (Fig. 3D-F); this mesodermal expression extends caudally with retraction of the node and is maintained through to formation of the notochord by 8.5 dpc (data not shown).

At 9.5 dpc, well after neural tube formation, strong expression of *Hhg-1* is seen in the entire notochord and in the ventral midline of caudal portions of the neural tube. More rostrally within the neural tube, *Hhg-1* expression extends ventrolaterally to encompass ~40% of the ventral neural tube at its maximum extent in the midbrain. Even more rostrally in the midbrain, midline expression is lost but reappears in a portion of the diencephalon (Fig. 4B). Horizontal sections demonstrate that expression rostral to the midbrain (Fig. 4C) splits and extends bilaterally (Fig. 4D,E), finally re-uniting in the ventral

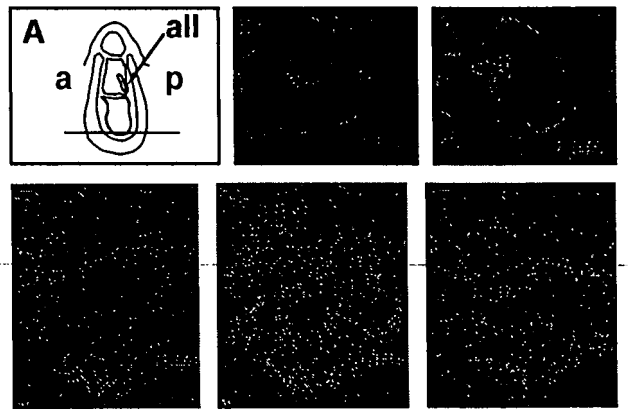

Fig. 3. *Hhg-1* expression at late gastrulation. (A) Schematic diagram showing 7.5 dpc mouse embryo, at late gastrulation. (B,C) Midsagittal sections through the egg cylinder showing hybridization in the axial mesoderm. (D-F) Adjacent horizontal sections through the egg cylinder at the level indicated in A. Note the hybridization in the midline mesoderm (asterisk). a, anterior; all, allantois; ect, ectoderm; mes, mesoderm; p, posterior.

midline of the diencephalon (Fig. 4B,E). *Hhg-1* expression thus is confined to a ring of cells in the ventral surface of the midbrain-diencephalic region. *Hhg-1* expression in the 10.5 dpc embryo is similar to that of the 9.5 dpc embryo, with strong expression in the notochord and most of the ventral neural tube and rostral neural tube expression remaining restricted to a ring of ventral cells. *Hhg-1* expression can also be observed in endoderm lining the future pharynx and foregut, with more intense expression occurring in the budding lungs; expression can also be detected in the hindgut. Finally, expression of *Hhg-1* in the limb buds at 10.5 dpc is restricted to the posterior margins of the forelimb (Fig. 5G-J) and hindlimb (data not shown). This expression clearly is restricted to the mesoderm and is absent from the overlying ectoderm, including the apical ridge. Our analysis of *Hhg-1* expression in the mouse embryo is consistent with that presented for *Shh* (Echelard et al., 1993) and for *vhh-1* in the rat embryo (Roelink et al., 1994).

Hhg-1 can function in *Drosophila* embryos

As a first step toward understanding the function of mouse *hedgehog* genes, we compared the effects of *Hhg-1* and *Drosophila hh* when ectopically expressed in *Drosopila* embryos under control of a heat inducible promoter. As described in Materials and Methods, germ-line insertions were made by P-element-mediated transformation of each gene cloned downstream of the *Drosophila* hsp70 promoter. Our analysis focused on one transformant line for each construct, designated hs*hh* and hs*Hhg-1*. Transcription of *hh* in the *Drosophila* embryo is normally restricted to a thin stripe of cells posterior to the parasegment boundary in each segment; expression of the *wingless* (*wg*) gene is normally restricted to a thin stripe of cells anterior and immediately adjacent to the *hh* stripe. Previous studies have demonstrated a dependence upon *hh* function for the maintenance of *wingless* expression (DiNardo et al., 1988; Martinez Arias et al., 1988); the spatial restriction of *wg* expression to this thin stripe is thought to result from limited diffusion of the signal encoded by *hh*. Ectopic expression of *hh* thus would be expected to cause an expansion in the domain of *wg* expression.

As shown in Fig. 6D,E, ubiquitous expression of *hh* induced by heat shock indeed causes an expansion in the extended germ band expression domain of the *wingless* gene, as has also been demonstrated by Ingham (1993). In addition, ectopic expression of *hh* produces consistent alterations in the size and orientation of denticles in the ventral cuticle (Fig. 6F; see Bejsovec and Wieschaus, 1993, for a description of the wild-type denticle pattern). The simplest interpretation of these changes is that bristle rows 4, 5 and 6 are replaced by bristles of size, shape and polarity normally associated with the denticles in rows 2 and 3, and our observations are again consistent with those of Ingham (1993). Neither of these changes occur in heat shocked wild-type embryos (Fig. 6A,C).

Similar analyses of ectopically expressed *Hhg-1* also reveal an expansion in the *wg* expression domain and effects upon the denticles in rows 4, 5 and 6 (Fig. 6G,I). The early effect on *wg*

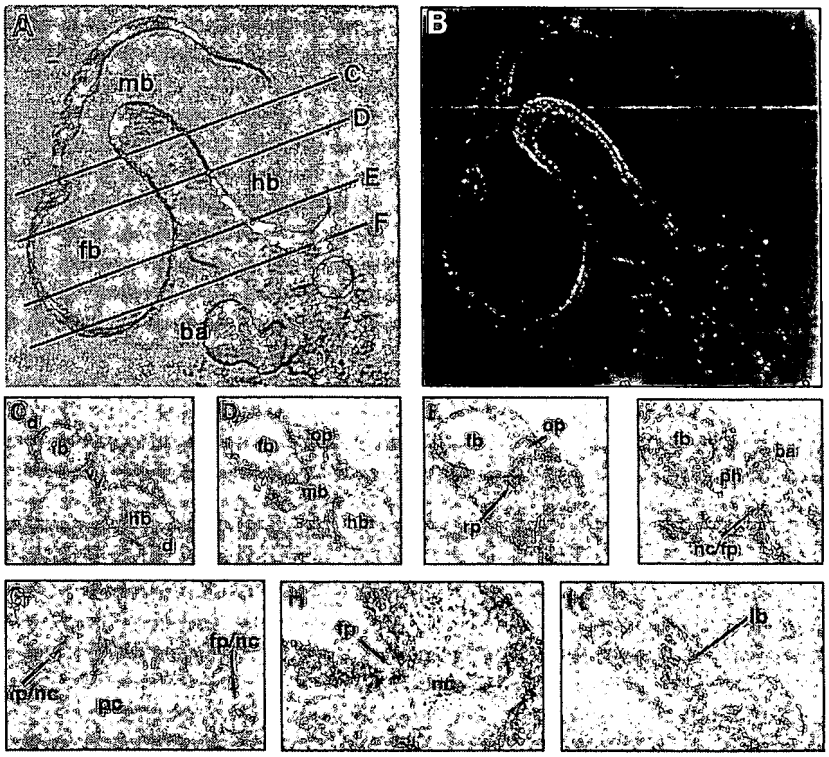

Fig. 4. *Hhg-1* expression in the 9.5 dpc embryo. (A,B) Bright and dark field views of a parasaggital section from a 9.5 dpc mouse embryo showing hybridization in the ventral midbrain and in a small patch of the ventral diencephalon. (C-F) Serial horizontal sections from superior to inferior levels in the head region of a 9.5 dpc mouse embryo. Broad, intense ventral hybridization is observed in the boundary region of the midbrain and forebrain (C). Rostrally, ventral-most expression is lost leaving two ventral/lateral domains of neural tube expression in cells adjacent to the optic vesicle. (D,E). Expression re-unites in a single midline domain of ventral neural tube cells overlying the pharyngeal lumen. Caudal to the hindbrain, neural tube expression is confined to the ventral midline (C-E) and expression is seen in the notochord beginning at its most rostral point (F). (G) Horizontal section at the level of the pericardiac region. The neural tube is cut twice in cross section at these levels and expression is likewise seen in floor plate and notochord of both cross sections. (H) Higher magnification view of G showing intense hybridization to floor plate and notochord. (I) Horizontal section at a lower level showing expression in the developing lung bud. In F, G and I, note the closer apposition of notochord to neural tube at more extreme rostral and caudal levels, indicative of an earlier stage of maturation relative to the intermediate level shown in H. ba, branchial arch; d, dorsal; fb, forebrain; fp, floor plate; lb, lung bud; mb, midbrain; nc, notochord; op, optic vesicle; pc, pericardiac region; ph, pharyngeal lumen; rp, Rathke's pouch; v, ventral.

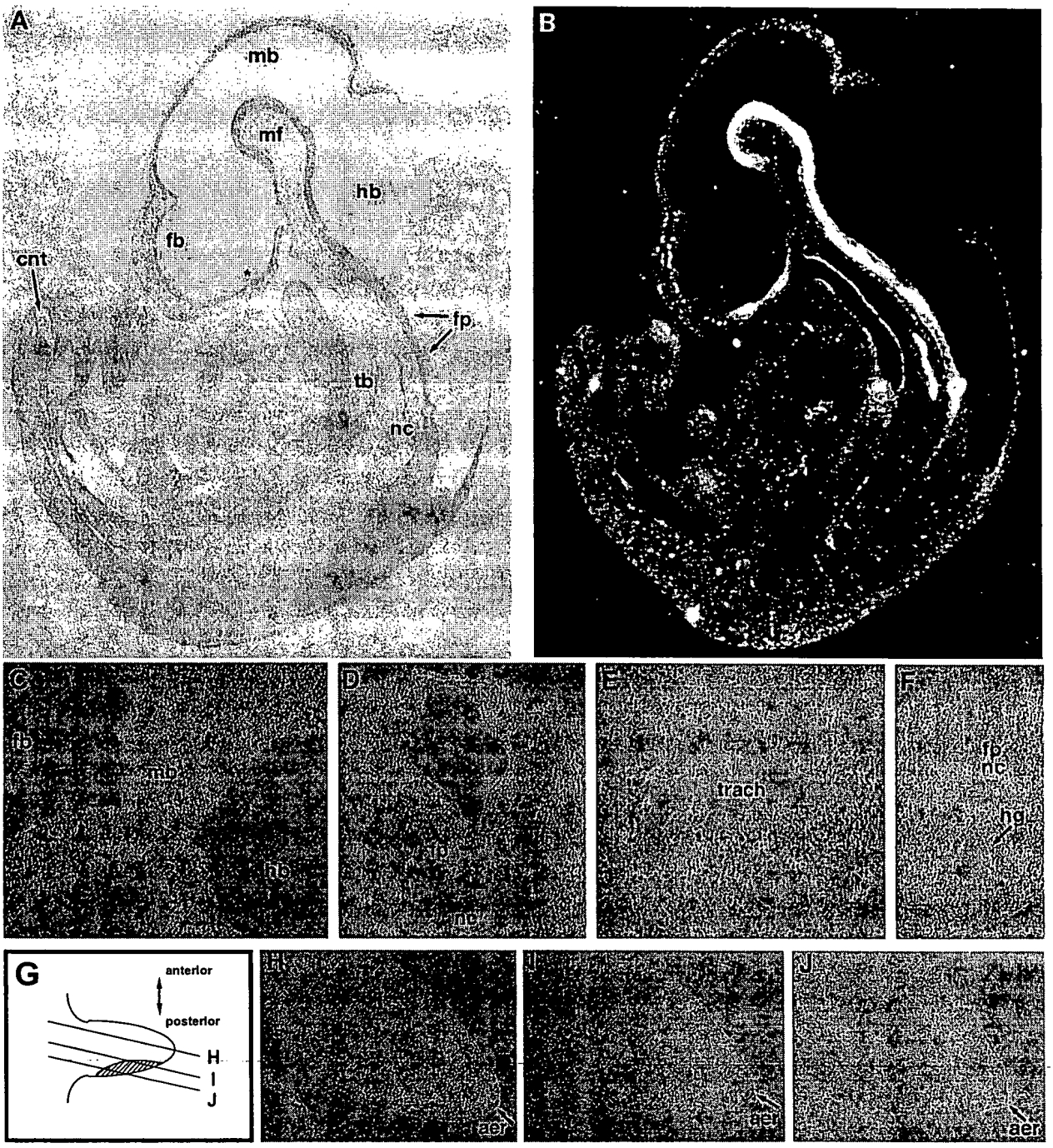

Fig. 5. *Hhg-1* expression in the 10.5 dpc embryo. (A,B) Bright-and dark-field views of a saggital section from a 10.5 dpc mouse embryo showing intense hybridization in the ventral neural tube and notochord, ventral diencephalic region (asterisk), and tracheal branch point. (C) Horizontal section showing hybridization in the ventral epithelium of the midbrain. (D) Horizontal section at lower level showing expression in floor plate and notochord. (E) Horizontal section showing hybridization in the epithelia of the tracheal lumen. (F) Horizontal section showing continued expression in the floor plate and notochord at caudal levels and expression in the epithelia of the hindgut. (G) Schematic diagram of developing limb, and reconstruction of expression from serial sections. Lines indicate approximate levels of sections shown in H-J. (H-J) Anterior to posterior sections of developing forelimb. Intense expression is observed in the posterior but not anterior mesoderm. No expression is observed in the apical ectodermal ridge. aer, apical ectodermal ridge; cnt, caudal neural tube; fb, forebrain; fp, floor plate; hb, hindbrain; hg, hindgut; mb, midbrain; mf, mesencephalic flexure; nc, notochord; tb, tracheal branch point; trach, tracheal lumen.

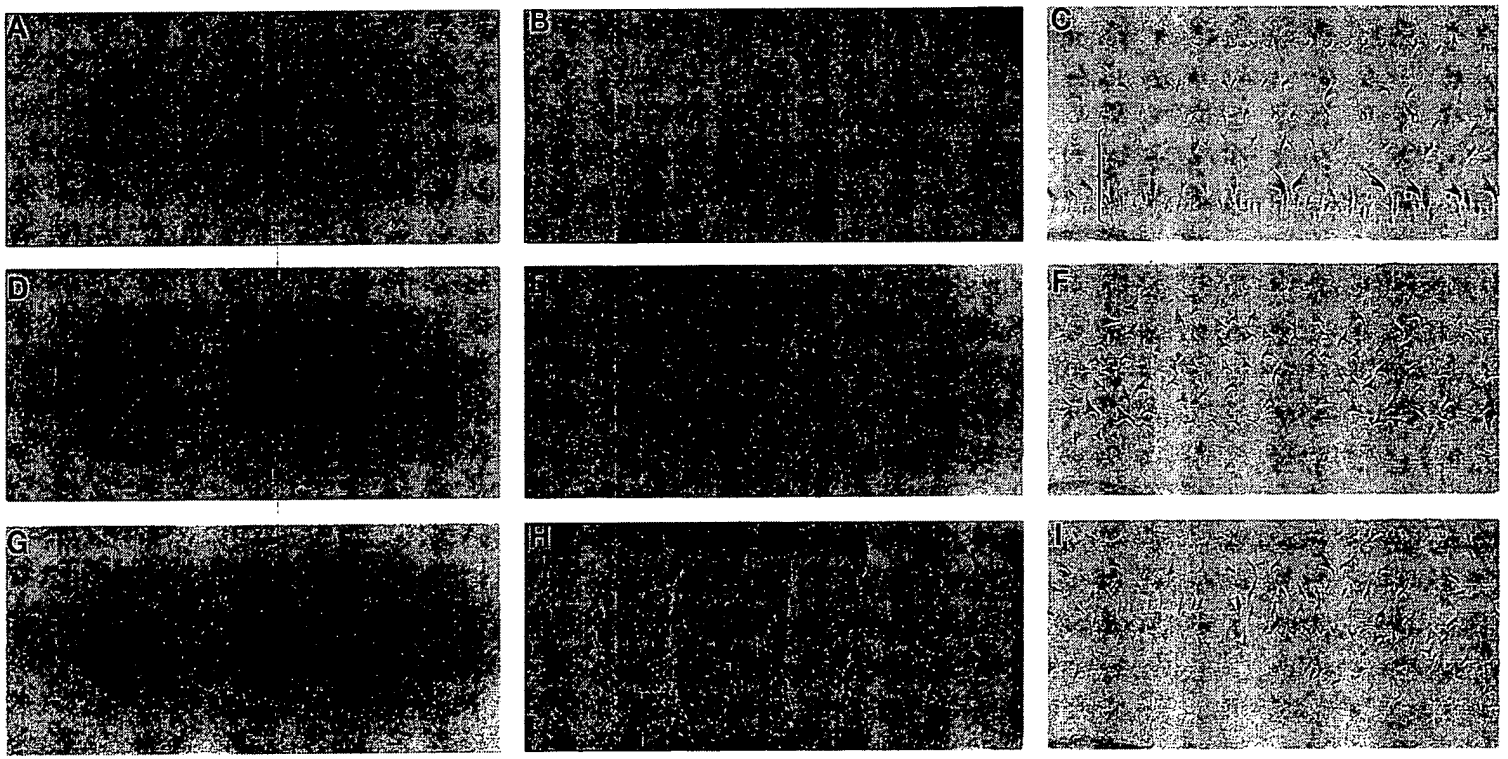

Fig. 6. Ectopic expression of *Hhg-1* in the *Drosophila* embryo. A,B,D,E,G and H show ventral views of germ-band-extended (A,D,G) and retracted (B,E,H) embryos which have been heat shocked and processed for in situ hybridization to detect *wingless* RNA expression. C, F and I show the pattern of ventral denticles within a single segment from heat-shocked embryos just prior to hatching. The genotypes of embryos in A-C are w^{1118} (wild-type control), while embryos in D-F and G-I, respectively, carry the hs*hh* and hs*Hhg-1* construct (see text). Note that, relative to wild type (A,B), the *wingless* stripes are expanded at the extended and retracted germ band stages for embryos carrying the hs*hh* (D,E) and hs*Hhg-1* (G,H) constructs. Note also that the wild-type polarity and character of the bristle rows 4-6 (bracketed portion of C; see text) are altered in F and I.

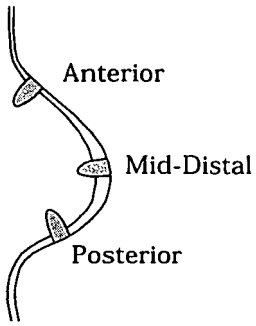

Fig. 7. Graft sites for limb patterning assays.

expression is indistinguishable from the *hh* effect. The denticles appearing in place of the posterior three denticle rows, however, appear more disorganized, with occasionally a missing denticle row and in some cases an unusual posterior row of anteriorly oriented denticles (Fig. 6I).

The patterns of *wg* expression thus far described pertain to the extended germ band stage. We also examined, however, the effects of ectopic *hh* and *Hhg-1* expression upon later stage embryos which had completed or nearly completed the process of germ band retraction. As shown in Fig. 6B,E,H, the *wg* expression domain is expanded relative to the wild type even at this later stage. The competence of cells in the expanded *wg* domain to respond to the ectopic *hh* signal at this late stage reveals a new requirement for temporal and spatial expression of candidate receptors for the *hh* signal (see Discussion).

Patterning activity of *Hhg-1* in the developing chick limb

Hhg-1 expression in mouse limb buds is restricted to mesoderm along the posterior margin of the limb bud (Fig. 5G-I), a location reminescent of the polarizing region in the chick limb bud. Given the ability of *Hhg-1* to function in as diverged a species as *Drosophila* (see above) and in light of previous reports of chick limb patterning activity present in grafts derived from mouse limb buds (Tickle et al., 1976; Fallon and Crosby, 1977), we tested the possibility that *Hhg-1* encodes an

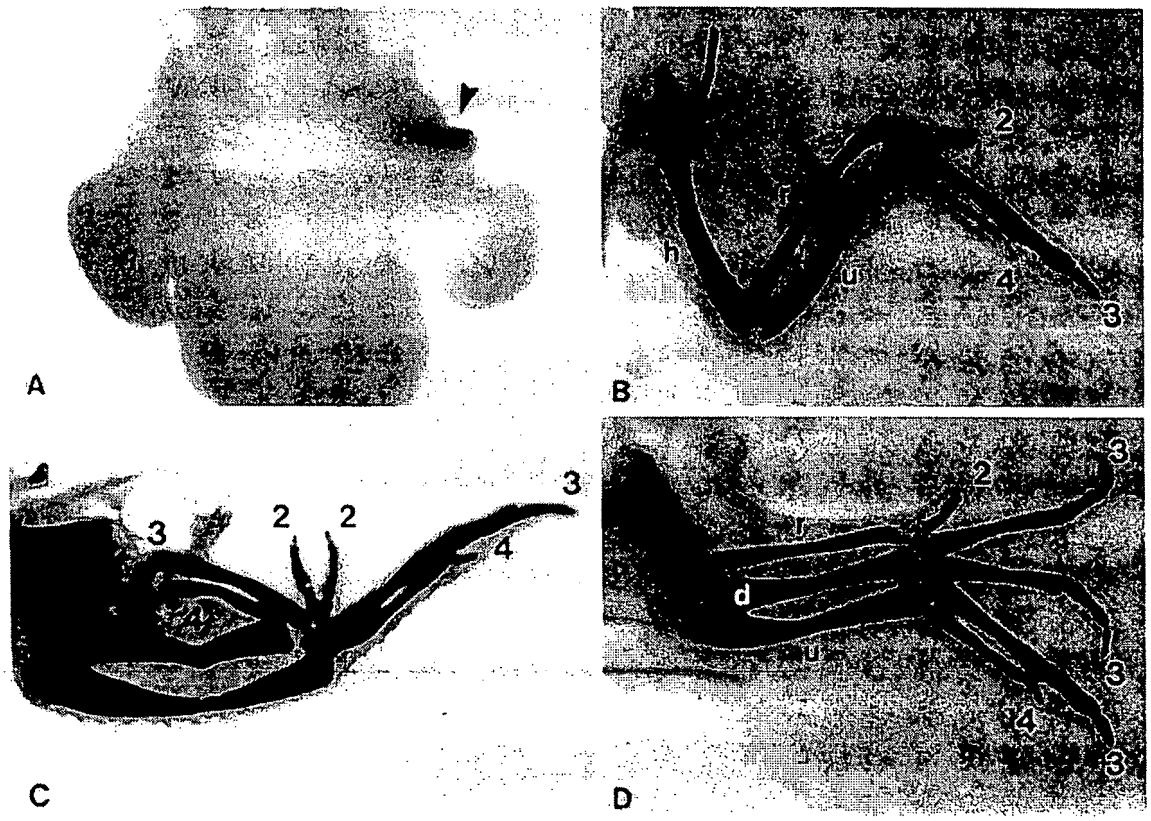

Fig. 8. Limb patterning activity of *Hhg-1*. Grafts of QT6 cells transfected with pCIS*lacZ* (A) or pCIS*Hhg-1* (B,C,D) were made to the anterior border (A,C) the posterior border (B) or to the mid-distal border (D) of forelimb buds within chick embryos at stage 20. The embryo in A was fixed 24 hours after grafting and stained for β-galactosidase activity (positive region indicated by arrowhead). Embryos in B-D were fixed, stained and cleared 7 days after grafting. The posterior border graft in B resulted in a normal limb skeleton (h, humerus; r, radius; u, ulna; 2,3 and 4 indicate digit identities). The anterior border graft in C caused a mirror image duplication of the manus with a digit pattern of 4-3-2-2-3-4. The mid-distal border graft in D induced skeletal duplications of digits and of the forearm: d indicates a duplicated forearm bone that probably is an ulna; the digit pattern from anterior is 2-3-3 followed by the normal 3-4.

activity capable of imposing pattern upon chick limbs. The strategy for these experiments involved high-efficiency transient transfection of the QT6 quail cell line (Moscovici et al., 1977), followed by grafting of wedge-shaped sections of transfected cell pellets to anterior, mid-distal or posterior borders of stage 20-21 chick wing buds (see Fig. 7). Initial transfections using the bacterial β-galactosidase expression gene in the vector pCIS (Gorman, 1985), which carries a cytomegalovirus promoter and an SV40 intron and polyadenylation signal, yielded expression in greater than 90% of the QT6 cells plated for transfection.

Fig. 8 shows that grafts of cells transfected with a *Hhg-1*-expression construct to anterior and mid-distal but not posterior locations within developing limb buds induced duplications of digits. Duplications induced by anterior border grafts were in mirror-image orientation relative to the normal pattern, with a typical sequence of digits shown in Fig. 8C (4-3-2-2-3-4). Mid-distal grafts commonly yielded digits in the sequence 2-3-3-3-4, with divergent curvature of adjacent third digits indicative of the location of the graft site (Fig. 8D). Grafts of β-galactosidase-expressing cells or posterior grafts of *Hhg-1*-expressing cells, in contrast, did not alter normal limb pattern (Fig. 8A,B). With respect to digit duplications and polarity, all grafts of *Hhg-1* expressing cells act as posterior organizing centers, much in the same manner observed for polarizing region grafts (Saunders and Gasseling, 1968).

Curiously, we observed duplications of proximal skeletal elements such as the humerus, radius and ulna at a frequency of 65% in mid-distal border grafts (Fig. 8D; see Table 1), but never with anterior border grafts (Fig. 8C; see Table 1). To our knowledge, a strong correlation between graft location and duplication of proximal skeletal elements has not been previously noted, although previously reported results are consistent with our observation (see Discussion). The overall level of proximal or distal element duplications in all limbs receiving anterior or mid-distal border grafts of *Hhg-1*-expressing cells was 86.5% (Table 1). These percentages are similar to those reported by Riddle et al. (1993) following anterior grafts of cells infected with a retrovirus carrying *Shh*, a *hedgehog* family member in the chicken that probably corresponds to *Hhg-1*.

Table 1. Skeletal element duplications induced by grafts of QT6 cells transfected with pCIS*Hhg-1*

Percentage of most posterior duplicated digit (*n*)				
Graft (*n*)	II	III	IV	Normal
Anterior hedgehog (29)	14% (4)	41% (12)	31% (9)	14% (4)
Mid-distal hedgehog (17)	17.5% (3)	65% (11)	0 (0)	17.5% (3)
β-galactosidase (11)	0	0	0	100% (11)
Posterior hedgehog (7)	0	0	0	100% (7)

Percentage of proximal element duplications* (*n*)				
Graft (*n*)	Radius	Ulna	Humerus	Normal
Anterior hedgehog (20)	0	0	0	100% (20)
Mid-distal hedgehog (17)	41% (7)	17.5% (3)	11.5% (2)	41% (7)
β-galactosidase (11)	0	0	0	100% (11)
Posterior hedgehog (7)	0	0	0	100% (7)

*A single specimen might contribute to more than one column.

Percentage of grafts that induced extra skeletal elements (*n*)		
Graft (*n*)	Duplications	Normal
Hedgehog (46)	87 % (40)†	13% (6)
β-galactosidase (11)	0	100% (11)
Posterior hedgehog (7)	0	100% (7)

†38 specimens showed digit duplications.

Qt6 cells transfected with either pCIS*Hhg-1* or pCIS*LacZ* were grafted to anterior, mid-distal or posterior borders of stage 20 chick limb buds. Embryos harvested at day 10 were fixed overnight in 10% formaldehyde, stained with Victoria Blue and cleared with methyl salicylate.

Proteolytic processing of the *Hhg-1* protein product

We have used affinity purified antibodies directed against epitopes from two distinct portions of the *Hhg-1* ORF (Fig. 9A) to confirm that *Hhg-1* encoded protein indeed is expressed in both systems where we have assayed for *Hhg-1* activity. As shown in the immunoblots of Fig. 9B, QT6 cells transfected with the pCIS*Hhg-1* expression vector produce a polypeptide species of ~45×10^3 M_r which is detected by both N- and C-terminal specific antibodies in transfected cells (lanes 1 and 3, respectively). In addition, a ~19×10^3 M_r species is specifically detected by the N-terminal antibody while the C-terminal antibody specifically detects a ~28×10^3 M_r species. Neither the

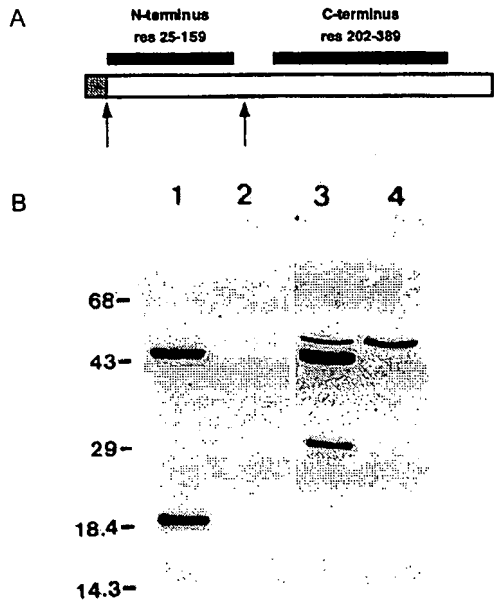

Fig. 9. Proteolytic processing of the *Hhg-1* protein. The filled boxes in A denote the portions of the *Hhg-1* ORF used to elicit antibodies, specific to the amino- and carboxy-terminal portions of the protein. The immunoblot in B illustrates the reactivity of amino-terminal (lanes 1 and 2) and carboxy-terminal (lanes 3 and 4) antibodies with species present in QT6 cells either transfected (lanes 1 and 3) or not transfected (lanes 2 and 4) with pCIS*Hhg-1*. Note the presence of a ~45×10^3 M_r transfection-dependent species detected by both antibodies. Each antibody also detects a single smaller species of ~19×10^3 M_r for the amino-terminal antibody and ~28×10^3 M_r for the carboxy terminal antibody. The slightly larger species detected in lanes 3 and 4 is not transfection dependent, but provides a control for the amount of protein loaded. The arrows in A denote a signal cleavage (following the shaded hydrophobic domain) and a proposed internal cleavage that can account for the observed species and their reactivities (see text).

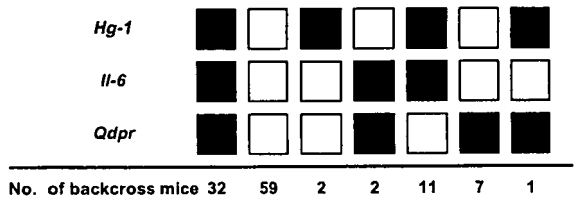

Fig. 10. Segregation of *Hhg-1* among proximal mouse chromosome 5 loci in [(C3H/HeJ-*gld* × *Mus spretus*)F1 × C3H/HeJ-*gld*] interspecific backcross mice Closed boxes represent the homozygous C3H pattern and open boxes the F_1 pattern. The number of mice with each haplotype is shown at the bottom of each column. The informative RFLV for *Hhg-1* is described in the text. The informative RFLVs for *Il-6* were generated by *Taq1* (C3H, 5.0 kb and 2.2 kb; *Mus spretus*, 8.6 kb and 1.9 kb) and for *Qdpr* were generated by *Eco*RI (C3H, 9.5 and 6.5 kb; *Mus spretus*, 8.2 kb).

large common species nor the smaller specific species are detected in untransfected cells (lanes 2 and 4). Essentially identical species were detected in protein extracts from heat shocked *Drosophila* embryos carrying the hs*Hhg-1* construct, but not in extracts from unshocked embryos (D. T. C. and P. A. B., data not shown).

The arrows in Fig. 9A denote cleavages of the primary protein product that could account for *Hhg-1* species of the observed size. The first of these occurs at the *Hhg-1* signal sequence and is observed in a microsome-dependent fashion in in vitro translation reactions (J. J. Lee and P. A. B., unpublished data). The second internal cleavage is proposed as a simple possibility that can account for the observed polypeptide species and is similar to an internal cleavage that occurs in the *Drosophila hedgehog* protein precursor (J. J. Lee, S. C. Ekker and P. A. B., unpublished; see Discussion).

Chromosomal localization and fine mapping of *Hhg-1*

In order to determine the chromosomal location of the *Hhg-1* gene and to assess potential linkage with mouse developmental mutants, we analyzed a panel of DNA samples from an interspecific cross that has been characterized for over 500 genetic markers throughout the genome. The genetic markers included in this map span between 50 and 60 centi-Morgans (cMs) on each mouse autosome and on the X Chromosome (for examples see Saunders and Seldin, 1990; Watson et al., 1992). Initially, DNA from the two parental mice [C3H/HeJ-*gld* and (c3H/HeJ-*gld* × *Mus spretus*)F_1] were digested with various restriction endonucleases and hybridized with *Hhg*-1 cDNA probe to determine restriction fragment length variants (RFLVs) thereby allowing haplotype analyses. Informative RFLVs were detected with *Msp*I restricted DNAs: C3H/HeJ-*gld*, 13.0 kb; *Mus spretus*, 5.0 kb. Comparison of the haplotype distribution of the *Hhg-1* indicated that in 109 of the 114 meiotic events examined, the *Hhg-1* locus cosegregated with Il-6 (Fig. 10), a locus previously mapped to proximal mouse Chromosome 5 (Mock et al., 1989; Kozak and Stephenson, 1993). The best gene order (Bishop, 1985) ± the standard deviation (Green, 1981) indicated the following gene order from proximal to distal: *Hhg-1* – 4.4 cM ± 1.9 cM – *Il-6* – 15.7 cM ± 3.5 cM – *Qdpr*.

DISCUSSION

Patterning functions of *Hhg-1*

The most remarkable feature of *Hhg-1* expression, which has also been noted for other closely related genes in multiple vertebrate species (Riddle et al., 1993; Echelard et al., 1993; Krauss et al., 1993; Roelink et al., 1994), is its occurrence in a number of embryonic tissues demonstrated to exert patterning influences on neighboring structures. The notochord and floor plate, for example, are capable of imposing ventral pattern upon the neural tube (reviewed in Jessell and Dodd, 1993), while the posterior margin of the vertebrate limb bud or polarizing region can function as a posterior organizing center when grafted to a developing limb. Grafting experiments also suggest that these organizing activities may be functionally related, since notochord and floor plate tissue can also function as posterior organizing centers when grafted to limb buds (Wagner et al., 1990).

Riddle et al. (1993) indeed showed that the chicken *Shh* gene encodes a product capable of imposing pattern upon developing chick limbs while Echelard et al. (1993) showed that ectopic expression of chicken *Shh* can induce inappropriate expression of ventral neural tube markers in the mouse; Krauss et al. (1993) also showed that ectopic expression of fish *shh* can induce inappropriate expression of ventral neural tube markers in fish embryos. Finally, Roelink et al. (1994) demonstrated that COS cells expressing the rat gene *vhh-1* can induce formation of floor plate and motor neurons when cocultured with lateral neural tube explants from rat.

The xenoplastic activities of *Hhg-1* described here represent the first direct assays of function for the mouse member of the *vhh-1* or *sonic* class of vertebrate *hh*-like sequences. Our results also demonstrate for the first time the activity of a mammalian *hh*-like gene in limb patterning. Consistent with the expression of *Hhg-1* in the posterior margin of mouse limb buds, polarizing activity previously has been identified in this location by grafting experiments (Tickle et al., 1976; Fallon and Crosby, 1977). In addition, preliminary results in the explant assay system suggest that the *Hhg-1* product can also induce floor plate formation in rat lateral neural tube (J. Dodd, D. T. C. and P. A. B., unpublished data). We thus conclude that the *Hhg-1* gene encodes patterning activities and that the expression of pattern of *Hhg-1* in the embryo could account, at least in part, for the patterning activities of specific tissues assayed by grafting experiments.

A noteworthy feature of our grafting operations was the high relative frequency of proximal skeletal element duplications in mid-distal grafts (65%) versus anterior grafts (0%). Although such a correlation between graft location and the occurrence of proximal duplications has not been previously noted, a cursory review of the literature from the first polarizing region grafts of Saunders and Gasseling (1968) onwards suggests that graft location indeed appears to operate as a determinant for formation of proximal element duplications. More recently, Riddle et al. (1993) reported proximal element duplications induced by anterior grafts of cells expressing the chicken *Shh* gene. In both cases of proximal element duplication depicted, however, the digit sequence indicated a location sufficiently posterior to allow formation at least one digit anterior to the graft, thus reinforcing the correlation between proximal

element duplications and a more posterior graft location (at least as far posterior as mid-distal). The significance of this observation remains to be investigated.

Genetic linkage of *Hhg-1*

Our segregation analysis of *Hhg-1* indicates a localization to the proximal region of mouse chromosome 5. Given the ability of *Hhg-1* to function in limb patterning, our attention was drawn to two mutations affecting limb development that also map to this region of mouse chromosome 5. One, *Hm* (hammertoe), is a semidominant mutation causing failure of normal programmed cell death in the webbing between toes during development, resulting in the formation of contractures in the second phalanx of all four limbs in the adult. This phenotype is somewhat more pronounced in homozygotes, which nevertheless remain viable and fertile. The second, *Hx* (Hemimelic extra toes), is also a dominant mutation associated with shortening or complete absence of tibia and talus in the hindlimbs and shortening of the radius in the forelimbs; in addition, metatarsals or metacarpals are duplicated giving a total of seven to eight digits per paw instead of the normal five (Dickie, 1968; Knudsen and Kochhar, 1981). The homozygous phenotype of *Hx* is an uncharacterized embryonic lethality (Knudsen and Kochhar, 1981). *Hx* and *Hm* are very closely linked but separate mutations, having been observed to recombine in only 1 of 3664 offspring from *trans*-heterozygous parents (Sweet, 1982). In addition to these mutations in the mouse, the syntenic region of human chromosome 7q has also been identified as the genetic locus for several developmental anomalies involving polydactyly (Tsukurov et al., 1994, Heutink et al., 1994).

In order to investigate the possibility that one or both of the mouse mutations affect the *Hhg-1* gene, we examined by Southern blotting the restriction pattern of DNA from both of these mutants. Using nine different restriction endonucleases for *Hx* and for *Hm*, we detected no differences between parental and mutant DNA (data not shown). Since the *Hx* phenotype suggests a defect in early limb patterning, as might be expected from a mutation in the *Hhg-1* gene, we attempted to discover alterations in *Hhg-1* coding sequences in the *Hx* mutant. Because only heterozygous *Hx* mutant DNA was available (from Jackson Labs), our conclusions depend upon analysis of multiple independently isolated clones. We examined eleven, fourteen and eight independent clones from the coding portions of exons one, two and three, respectively, without detecting any differences from wild type (see Materials and Methods). Since the clones for sequence determination were derived using the polymerase chain reaction, it is possible that a deletion(s) at the *Hhg-1* locus might have prevented amplification of the mutant allele. Given the uncertainty inherent in sampling from heterozygous DNA, it is also formally possible, although highly unlikely, that we could have missed a coding difference in the *Hhg-1* gene of *Hx* mutants.

In the absence of *Hx*- or *Hm*-associated alterations in *Hhg-1* coding sequence, another possibility to consider is that the *Hx* or *Hm* phenotypes could result from a mutation in *cis*-acting regulatory regions of *Hhg-1*, causing either a reduction of *Hhg-1* expression or inappropriate spatial localization of expression. Given our Southern blotting results, such a lesion could lie near the *Hhg-1* gene only if it is sufficiently subtle to escape detection by Southern blotting with our cDNA probe; alternatively, a *Hhg-1* regulatory lesion may have escaped detection because of a location distant from sequences represented within the *Hhg-1* cDNA.

With regard to potential mechanisms underlying genetic dominance for such a regulatory mutation, the dominant limb deformity mutation *Xt* (extra toes) may be informative. Like *Hx*, *Xt* causes polydactyly and is lethal when homozygous; mutations affect the gene GLI3, which encodes a zinc finger transcription factor. At least one allele of *Xt* appears to act simply by disrupting transcription of GLI3 (Schimmang et al., 1992), and thus, the genetic dominance of mutations at this locus is probably due to haploinsufficiency. The GLI3 gene is also interesting in that its close *Drosophila* relative, the gene *cubitus-interruptus*^{Dominant} (*ci*^{D}), functions downstream in the *hedgehog* signaling pathway (Forbes et al., 1993). If the GLI3 gene similarly functions downstream of *Hhg-1* in the mouse, and given that GLI3 function is haploinsufficient, it would not be surprising to find that partial loss of *Hhg-1* expression caused by a regulatory mutation might also have a dominant phenotype. Interestingly, a human polysyndactyly disease that maps to a region of human chromosome 7 syntenic to the region containing *Hhg-1* and *Hm* and *Hx* is also inherited in a dominant fashion (Tsukurov et al., 1994; Heutink et al., 1994). Alternatives to haploinsufficiency are that a regulatory mutation might cause *Hhg-1* mis-expression or that *Hx* and *Hm* are unrelated to *Hhg-1*.

Duplication and divergence of the *hedgehog* gene family in vertebrates

Our PCR-based search for vertebrate *hedgehog* homologues yielded the three distinct mouse and two distinct human sequences reported here, and five sequences each from the zebrafish *Brachydanio rerio* and the toad *Xenopus laevis* (S. C. Ekker, J. J. Lee, D.v.K. and P. A. B., unpublished data). In contrast, none of the invertebrate species to which our PCR-based method was applied yielded more than a single distinct *hh*-like sequence. For example, using various combinations of degenerate primers from conserved regions, eighteen independent *Drosophila melanogaster* clones identical to *hh* were isolated without encountering any diverged *hh*-like sequences. It is not yet possible to estimate accurately the total number of distinct vertebrate *hh*-like genes. The occurrence of multiple *hh*-like sequences in vertebrates but not invertebrates nevertheless suggests that at some point during evolution of the vertebrate lineage repeated duplication and divergence of a single ancestral *hedgehog* gene occurred, as has been proposed for the origin of multiple vertebrate HOM-C gene clusters from a single ancestral cluster (Schubert et al., 1993).

Broad evolutionary conservation of *hedgehog* protein function and proteolytic processing

The evolutionary conservation of *hh* extends beyond sequence to include function, as demonstrated by the ability of *Hhg-1* to encode a signal capable of inducing expansion of the *wingless* stripe of expression in *Drosophila* embryos. Similar results using a *hh*-like gene isolated from zebrafish were also reported by Krauss et al. (1993). If the proposal, based on genetic arguments, that the gene *patched* (*ptc*) encodes a *hh* receptor in *Drosophila* is correct (Ingham et al., 1991), the functional conservation of vertebrate *hedgehog* signals would suggest that *ptc*-like sequences and function should also be conserved in

vertebrates. With regard to the identity of a *hh* receptor, however, we observed that both *hh* and *Hhg-1* can induce broadening of the *wingless* stripe when ectopically expressed at the retracted germ band stage of *Drosophila* development. By this stage, the initially broad stripe of *ptc* mRNA and protein expression has split into two thinner stripes per segment by loss of expression from the cells in the middle of the broad stripe (Taylor et al., 1993). Expanded *wingless* expression in response to *hh* thus is occurring in interstripe cells that in normal embryos no longer express the *ptc* protein. Ingham (1993) has reported that *ptc* expression in these interstripe cells is also induced by ectopic *hedgehog*, but it is not known whether *ptc* induction in the interstripe precedes or follows *wg* induction in the interstripe cells. Whatever the sequence of induction, novel expression of *ptc* or *wg* represents a response to *hh* protein in interstripe cells, which do not express the *ptc* protein, thus suggesting that *ptc* does not encode the *hh* receptor, or at least not the only receptor.

The occurrence of multiple *Hhg-1* polypeptide species in *Drosophila* embryos as well as in avian cells raises a question as to the role of proteolytic processing in *hedgehog* protein function. We believe that the N- and C-terminally derived forms of the *Hhg-1* protein bear a product/precursor relationship to the larger form because the relative molecular masses of the smaller products sum to yield approximately the relative molecular mass of the larger product, and they could therefore be derived by a single internal cleavage as shown in the model in Fig. 9A. The location of this internal cleavage coincides approximately with an intron/exon boundary and with a sharp demarcation in the degree of sequence conservation (see Results). In addition, these smaller forms resemble smaller forms of the *hh* protein observed in *Drosophila* (Tabata and Kornberg, 1994; J. J. Lee and P. A. B., unpublished data), where an internal cleavage occurs and appears to be required for the *hh* signaling function (J. J. Lee, S. C. Ekker, D. P. von K. and P. A. B., unpublished data).

The existence of two distinct stable products derived from a single larger precursor may provide a clue to the apparent dual nature of *hedgehog* gene action in several developmental systems. In the *Drosophila* embryo, for example, the restriction of *wingless* gene expression to a narrow stripe within each segment is dependent upon the short-range nature of a *hedgehog* signaling activity (see above; Ingham, 1993); in contrast, the influence of a later-acting *hh*-encoded activity extends across most of the segment in imposing pattern upon the dorsal cuticle (Heemskerk and DiNardo, 1994). Similarly in ventral neural tube patterning, induction of floor plate occurs at short range and depends upon direct contact with notochord, floor plate, or COS cells expressing *vhh-1* (Placzek et al., 1993; Roelink et al., 1994). COS cells expresssing *vhh-1* also have motor neuron inducing activity (Roelink et al., 1994). This latter activity is found in diffusible form in supernatants from notochord and floor plate cultures (Yamada et al., 1993), although it is not yet clear that *vhh-1* directly encodes the diffusible activity. Long- and short-range *hedgehog* activities have not been definitively identified in the context of limb patterning, but such activities have been extensively discussed; dual modes of *hedgehog* action thus may yet emerge from studies of such apparently distinct activities as influences upon the apical ectodermal ridge and anterior/posterior patterning of the developing limb.

An alternative would be that only one of the smaller *hedgehog* protein species is biologically active, with the apparent dual nature of *hedgehog* action deriving from secondary effects. For example, restricted diffusion for the primary active species could produce apparent long-range effects by inducing expression of another diffusible molecule. Similarly, a diffusible or primarily long-range *hedgehog* signal could yield apparent short-range effects through threshhold-dependent responses of target cells. To resolve these questions, the structures and embryonic localizations of the *hedgehog*-encoded proteins must be determined and their patterning activities assayed. At another level, a true understanding of the functional roles of vertebrate *hedgehog* proteins requires a demonstration that patterning functions in vertebrate embryos actually are executed by the products of this class of genes; this would best be achieved through specific inactivation of *hedgehog* gene products by genetic or other means.

We gratefully acknowledge J. Gearhart, S.-J. Lee, C. Moore, C. Mjaatvedt and T. Huynh for instruction in handling of mice, manipulation of embryos, and advice on in situ hybridisation. We also thank A. Lanahan, J. Williams and S.-J. Lee for mouse cDNA libraries and RNA blots. K. Young, M. Claudia, D. Sullivan, J. Kassis, S. Brown, R. Denell, G. Aisenberg and A. Cameron generously provided genomic DNA and libraries from various species, and K. Young graciously assisted in the isolation and characterization of the mosquito and mouse sequences. We are indebted to N. Patel for equipment and help with dark field microscopy. We also thank J. Dodd, J. J. Lee and S. C. Ekker, for sharing unpublished data, and S.C. Ekker for help with figures. T. Vogt and S.-J. Lee provided useful comments on the manuscript. This work was supported by the Howard Hughes Medical Institute, an NIH MSTP award to D. T. C., NIH awards HD20743 and 5T32GM07507 to J. F. F. and A. L., and NIH award HG00734 to M. F. S.

REFERENCES

Ausubel, F. M., Brent, R., Kingston, R. E., Moore, D. D., Seidman, J. G., Smith, J. A. and Struhl, K. (1993). *Current Protocols in Molecular Biology*. New York: Greene Publishing Associates and Wiley-Interscience.

Baker, N. E. (1988). Embryonic and imaginal requirements for *wingless*, a segment polarity gene in *Drosophila*. *Dev. Biol.* **125**, 96-108.

Bejsovec, A. and Martinez-Arias, A. (1991). Roles of *wingless* in patterning the larval epidermis of *Drosophila*. *Development* **113**, 471-485.

Bejsovec, A. and Wieschaus, E. (1993). Segment polarity gene interactions modulate epidermal patterning in *Drosophila* embryos. *Development* **119**, 501-517.

Bishop, D. T. (1985). The information content of phase-known matings for ordering genetic loci. *Genet. Epidemiol.* **2**, 349-361.

Burnette, W. N. (1981). Western blotting: electrophoretic transfer of proteins from sodium dodecyl sulfate-polyacrylamide gels to unmodified nitrocellulose and radiographic detection with antibody and radio-iodinated Protein A. *Anal. Biochem* **112**, 195-203.

Chen, C. and Okayama, H. (1987). High-efficiency transformation of mammalian cells by plasmid DNA. *Molecular & Cellular Biology* **7**, 2745-2752.

Dickie, M. M. (1968). *Mouse News Lett.* **38**, 24.

DiNardo, S., Sher, E., Heemskerk-Jongens, J., Kassis, J. A. and O'Farrell, P. H. (1988). Two-tiered regulation of spatially patterned *engrailed* gene expression during *Drosophila* embryogenesis. *Nature* **332**, 604-609.

Dougan, S. and DiNardo, S. (1992). *Drosophila wingless* generates cell type diversity among *engrailed* expressing cells. *Nature* **360**, 347-50.

Echelard, Y., Epstein, D. J., St-Jacques, B., Shen, L., Mohler, J., McMahon, J. A. and McMahon, A. P. (1993). Sonic hedgehog, a member of a family of putative signaling molecules, is implicated in the regulation of CNS polarity. *Cell* **75**, 1417-1430.

Fallon, J. F. and Crosby, G. M. (1977). Polarizing zone activity in limb buds

of amniotes. In *Vertebrate Limb and Somite Morphogenesis*. (ed. D. A. Ede, J. R. Hinchliffe and M. Balls), pp 55-70. Cambridge: England.

Feinberg, A. and Vogelstein, B. (1983). A technique for radiolabeling DNA restriction endonuclease fragments to high specific activity. *Anal. Biochem.* **132**, 6-13.

Ferguson, E. L. and Anderson, K. V. (1992). Decapentaplegic acts as a morphogen to organize dorsal-ventral pattern in the Drosophila embryo. *Cell* **71**, 451-461.

Forbes, A. J., Nakano, Y., Taylor, A. M. and Ingham, P. W. (1993). Genetic analysis of *hedgehog* signalling in the *Drosophila* embryo. *Development* **1993 Supplement**, 115-124.

Gorman, C. (1985). High efficiency gene transfer into mammalian cells. In *DNA cloning*. (ed. D. M. Glover). pp 143. Oxford.

Green, E. L. (1981). Linkage, recombination and mapping. In *Genetics and Probability in Animal Breeding Experiments*. (ed. E. Green), pp 77-113. New York.

Harlow, E. and Lane, D. (1988). *Antibodies: A Laboratory Manual*. Cold Spring Harbor, New York: Cold Spring Harbor Publications.

Heberlein, U., Wolff, T. and Rubin, G. M. (1993). The TGF beta homolog *dpp* and the segment polarity gene *hedgehog* are required for propagation of a morphogenetic wave in the Drosophila retina. *Cell* **75**, 913-926.

Heemskerk, J. and DiNardo, S. (1994). Drosophila *hedgehog* acts as a morphogen in cellular patterning. *Cell* **76**, 449-460.

Heutink, P., Zguricas, J., Oosterhout, L. v., Breedveld, G. J., Testers, L., Sandkuijl, L. A., Snijders, P. J. L. M., Weissenbach, J., Lindhout, D., Hovius, S. E. R. and Oostra, B. A. (1994). The gene for triphalangeal thumb maps to the subtelomeric region of chromosome 7q. *Nature Genetics* **6**, 287-292.

Ingham, P. W. (1993). Localized *hedgehog* activity controls spatial limits of wingless transcription in the *Drosophila* embryo. *Nature* **366**, 560-562.

Ingham, P. W., Taylor, A. M. and Nakano, Y. (1991). Role of the *Drosophila patched* gene in positional signalling. *Nature* **353**, 184-187.

Jessell, T. M. and Dodd, J. (1993). Control of neural cell identity and pattern by notochord and floor plate signals. In *Cell-Cell Signaling in Vertebrate Development*. (ed. E. J. Robertson, F. R. Maxfield and H. J. Vogel), pp 139-155. Sand Diego.

Knudsen, T. B. and Kochhar, D. M. (1981). The role of morphogenetic cell death during abnormal limb-bud outgrowth in mice heterozygous for the dominant mutation *Hemimelia-extra toe* (*Hmx*). *J. Embryol. Exp. Morphol* **65 (Supplement)**, 289-307.

Kozak, C. A. and Stephenson, D. A. (1993). Mouse chromosome 5. *Mammalian Genome* **4**, s72-87.

Krauss, S., Concordet, J.-P. and Ingham, P. W. (1993). A functionally conserved homolog of the Drosophila segment polarity gene *hh* is expressed in tissues with polarizing activity in zebrafish embryos. *Cell* **75**, 1431-1444.

Laemmli, U. K. (1970). Cleavage of structural proteins during the assembly of the head of bacteriophage T4. *Nature* **227**, 680-685.

Lee, J. J., von Kessler, D. P., Park, S. and Beachy, P. A. (1992). Secretion and localized transcription suggest a role in positional signaling for products of the segmentation gene hedgehog. *Cell* **71**, 33-50.

Lee, S. J. (1990). Identification of a novel member (GDF-1) of the transforming growth factor-β superfamily. *Mol. Endocrinol.* **4**, 1034-1040.

Lockyer, J., Cook, R. G., Milatien, S., Kaufman, S., Woo, S. L. C. and Ledley, F. D. (1987). Structure and expression of human dihydropteridine reductase. *Proc. Natl. Acad. Sci. USA* **84**, 3329-3333.

Ma, C., Zhou, Y., Beachy, P. A. and Moses, K. (1993). The segment polarity gene *hedgehog* is required for progression of the morphogenetic furrow in the developing *Drosophila* eye. *Cell* **75**, 927-938.

Martinez Arias, A., Baker, N. E. and Ingham, P. W. (1988). Role of segment polarity genes in the definition and maintenance of cell states in the *Drosophila* embryo. *Development* **103**, 157-170.

Mock, B. A., Nordan, R. P., Justice, M. J., Kozak, C., Jenkins, N. A., Copeland, N. G., Clark, S. C., Wong, G. G. and Rudikoff, S. (1989). The murine Il-6 gene maps to the proximal region of Chromosome 5. *Journal of Immunology* **142**, 1372-1376.

Mohler, J. (1988). Requirements for *hedgehog*, a segmental polarity gene, in patterning larval and adult cuticle of *Drosophila*. *Genetics* **120**, 1061-1072.

Mohler, J. and Vani, K. (1992). Molecular organization and embryonic expression of the hedgehog gene involved in cell-cell communication in segmental patterning in Drosophila. *Development* **115**, 957-971.

Moscovici, C., Moscovici, M. G., Jimenez, H., Lai, M. M., Hayman, M. J. and Vogt, P. K. (1977). Continuous tissue culture cell lines derived from chemically induced tumors of Japanese quail. *Cell* **11**, 95-103.

Nusse, R. and Varmus, H. E. (1992). *Wnt* genes. *Cell* **69**, 1073-1087.

Peifer, M. and Bejsovec, A. (1992). Knowing your neighbors: cell interactions determine intrasegmental patterning in Drosophila. *Trends in Genetics* **8**, 243-249.

Placzek, M., Jessell, T. M., and Dodd, J. (1993). Induction of floor plate differentiation by contact-dependent homeogenetic signals. *Development* **117**, 205-218.

Riddle, D. R., Johnson, R. L., Laufer, E. and Tabin, C. (1993). Sonic hedgehog mediates the polarizing activity of the ZPA. *Cell* **75**, 1401-1416.

Rijsewijk, F., Schuermann, M., Wagenaar, E., Parren, P., Weigel, D. and Nusse, R. (1987). The Drosophila homolog of the mouse mammary oncogene *int-1* is identical to the segment polarity gene *wingless*. *Cell* **50**, 649-657.

Riley, B. B., Savage, M. P., Simandl, B. K., Olwin, B. B. and Fallon, J. F. (1993). Retroviral expression of FGF-2 (bFGF) affects patterning in chick limb bud. *Development* **118**, 95-104.

Roelink, H., Augsburger, A., Heemskerk, J., Korzh, V., Norlin, S., Ruiz i Altaba, A., Tanabe, Y., Placzek, M., Edlund, T., Jessell, T. M. and Dodd, J. (1994). Floor plate and motor neuron induction by *vhh-1*, a vertebrate homolg of *hedgehog* expressed by the notochord. *Cell* **76**, 761-775.

Rubin, G. M. and Spradling, A. C. (1982). Genetic transformation of Drosophila with transposable element vectors. *Science* **218**, 348-353.

Sambrook, J., Fritsch, E. F. and Maniatis, T. (1989). Molecular Cloning: A Laboratory Manual. 2nd edition Cold Spring Harbor, Cold Spring Harbor Laboratory Publications.

Sanger, F., Nicklen, S. and Coulson, A. R. (1977). DNA sequencing with chain-terminating inhibitors. *Proc. Natl. Acad. Sci. USA* **74**, 5463-5467.

Saunders, A. M. and Seldin, M. F. (1990). A molecular genetic linkage map of mouse chromosome 7. *Genomics* **8**, 524-535.

Saunders, J. W. and Gasseling, M. (1968). Ectodermal-mesenchymal interaction in the origin of limb symmetry. In *Epithelial-Mesenchymal Interaction*. (ed. R. Fleischmayer and R. E. Billingham), pp 78-97. Baltimore.

Schimmang, T., Lemaistre, M., Vortkamp, A. and Ruther, U. (1992). Expression of the zinc finger gene *Gli3* is affected in the morphogenetic mouse mutant *extra-toes* (*Xt*). *Development* **116**, 799-804.

Schubert, F. R., Nieselt-Struwe, K. and Gruss, P. (1993). The Antennapedia-type homeobox genes have evolved from three precursors separated early in metazoan evolution. *Proc. Natl. Acad. Sci. USA* **90**, 143-147.

Seldin, M. F., Morse, H. C., Reeves, J. P., Scribner, J. P., LeBoeuf, R. C. and Steinber, A. D. (1988). Genetic analysis of autoimmune *gld* mice I. Identification of a restriction fragment length polymorphism closely linked to the *gld* mutation within a conserved linkage group. *J. Exp. Med.* **167**, 688-693.

Sweet, H. O. (1982). *Mouse News Lett.* 66, 66.

Tabata, T., Eaton, S. and Kornberg, T. (1992). The Drosophila *hedgehog* gene is expressed specifically in posterior compartment cells and is a target of *engrailed* regulation. *Genes Dev.* **6**, 2635-2645.

Tabata, T. and Kornberg, T. B. (1994). *Hedgehog* is a signaling protein with a key role in patterning *Drosophila* imaginal discs. *Cell* **76**, 89-102.

Tashiro, S., Michiue, T., Higashijima, S., Zenno, S., Ishimaru, S., Takahashi, F., Orihara, M., Kojima, T. and Saigo, K. (1993). Structure and expression of *hedgehog*, a *Drosophila* segment polarity gene required for cell-cell communication. *Gene* **124**, 183-189.

Tautz, D. and Pfeifle, C. (1989). A non-radioactive *in situ* hybridization method for the localization of specific RNAs in the *Drosophila* embryo reveals translational control of the segmentation gene *hunchback*. *Chromosoma* **98**, 81-85.

Taylor, A. M., Nakano, Y., Mohler, J. and Ingham, P. W. (1993). Contrasting distributions of *patched* and *hedgehog* proteins in the *Drosophila* embryo. *Mech. Dev.* **42**, 89-96.

Thummel, C. S., Boulet, A. M. and Lipshitz, H. D. (1988). Vectors for *Drosophila* P-element-mediated transformation and tissue culture transfection. *Gene* **74**, 445-456.

Tickle, C., Shellswell, G., Crawley, A. and Wolpert, L. (1976). Positional signalling by mouse limb polarising region in the chick wing bud. *Nature* **259**, 396-397.

Tsukurov, O., Boehmer, A., Flynn, J., Nicolai, J.-P., Hamel, B. C. J., Traill, S., Zaleske, D., Mankin, H. J., Yeon, H., Ho, C., Tabin, C., Seidman, J. G. and Seidman, C. (1994). A complex bilateral polysyndactyly disease locus maps to chromosome 7q36. *Nature Genetics* **6**, 282-286.

von Heijne, G. (1986). A new method for predicting signal sequence cleavage sites. *Nucl. Acids Res.* **14**, 4683-4690.

Wagner, M., Thaller, C., Jessell, T. and Eichele, G. (1990). Polarizing activity and retinoid synthesis in the floor plate of the neural tube. *Nature* **345**, 819-822.

Watson, M. L., D'Eustachio, P. D., Mock, B. A., Steinberg, A. D., Morse, H. C. I., Oakey, R. J., Howard, T. A., Rochelle, J. M. and Seldin, M. F. (1992). A linkage map of mouse chromosome 1 using an interspecific cross segregating for the gld autoimmunity mutation. *Mammalian Genome* **2**, 158-171.

Wieschaus, E. and Nusslein-Volhard, C. (1986). Looking at embryos. In *Drosophila: A Practical Approach*. (ed. D. B. Roberts), pp 199-227. Oxford: England.

Wilkinson, D. G. (1992). Whole mount *in situ* hybridization of vertebrate embryos. In *In situ hybridization: A practical approach*. (ed. D. G. Wilkinson), pp 75-83. Oxford.

Wolpert, L. (1969). Positional information and the spatial pattern of cellular differentiation. *Journal of Theoretical Biology* **25**, 1-47.

Yamada, T., Pfaff, S. L., Edlund, T., and Jessell, T. M. (1993). Control of cell pattern in the neural tube: motor neuron induction by diffusible factors from notochord and floor plate. *Cell* **73**, 673-686.

(Accepted 12 August 1994)